The generalized Thévenin equivalent representation becomes

$$\hat{V}(0) = -\underbrace{\begin{bmatrix} \hat{Z}_{S1} + \hat{Z}_{S0} & \hat{Z}_{S0} \\ \hat{Z}_{S0} & \hat{Z}_{S2} + \hat{Z}_{S0} \end{bmatrix}}_{\hat{Z}_S} \hat{I}(0) = -\underbrace{\begin{bmatrix} 75 + j0 & 25 + j25 \\ 25 + j25 & 125 + j125 \end{bmatrix}}_{\hat{Z}_S} \hat{I}(0)$$

$$\hat{V}(\mathscr{L}) = \underbrace{\begin{bmatrix} \hat{Z}_{L1} + \hat{Z}_{L0} & \hat{Z}_{L0} \\ \hat{Z}_{L0} & \hat{Z}_{L2} + \hat{Z}_{L0} \end{bmatrix}}_{\hat{Z}_L} \hat{I}(\mathscr{L}) = \underbrace{\begin{bmatrix} 200 - j25 & 150 - j50 \\ 150 - j50 & 250 - j100 \end{bmatrix}}_{\hat{Z}_L} \hat{I}(\mathscr{L})$$

The results computed by Harrison are

$$\beta\mathscr{L} = 1.5 \begin{cases} I_0(0) = 6.255E-5 \text{ A}, & I_0(\mathscr{L}) = 3.650E-5 \text{ A} \\ I_1(0) = 1.065E-5 \text{ A}, & I_1(\mathscr{L}) = 1.220E-5 \text{ A} \\ I_2(0) = 5.644E-5 \text{ A}, & I_2(\mathscr{L}) = 2.784E-5 \text{ A} \end{cases}$$

The results computed by the program **WIRE** described in [H.1] are

$$\beta\mathscr{L} = 1.5 \begin{cases} I_1(0) = 1.066E-5\underline{/-99.83^\circ} \text{ A}, & I_1(\mathscr{L}) = 1.221E-5\underline{/158.65^\circ} \text{ A} \\ I_2(0) = 5.647E-5\underline{/-159.07^\circ} \text{ A}, & I_2(\mathscr{L}) = 2.784E-5\underline{/-148.26^\circ} \text{ A} \end{cases}$$

The results computed from the distributed source MTL model described herein using the code **INCIDENT.FOR** described in Appendix A are

$$\beta\mathscr{L} = 1.5 \begin{cases} I_1(0) = 1.066E-5\underline{/-99.83^\circ} \text{ A}, & I_1(\mathscr{L}) = 1.221E-5\underline{/158.65^\circ} \text{ A} \\ I_2(0) = 5.647E-5\underline{/-159.07^\circ} \text{ A}, & I_2(\mathscr{L}) = 2.784E-5\underline{/-148.26^\circ} \text{ A} \end{cases}$$

which correspond well to Harrison's results.

The last example is the case of two wires above an infinite ground plane illustrated in Fig. 7.16 which was considered in [H.1]. Wire #1 has a radius of 30 mils and is located at $y = 0$ and height above ground of 5 cm. Wire #2 has a radius of 10 mils and is located at $y = 4$ cm and height above ground of 2 cm. The line length is 1 m and $\hat{Z}_{S1} = 100\,\Omega$, $\hat{Z}_{L1} = 500\,\Omega$, $\hat{Z}_{S2} = 500\,\Omega$, and $\hat{Z}_{L2} = 1000\,\Omega$. This results in a generalized Thévenin equivalent characterization of the terminations as

$$\hat{V}(0) = -\underbrace{\begin{bmatrix} \hat{Z}_{S1} & 0 \\ 0 & \hat{Z}_{S2} \end{bmatrix}}_{\hat{Z}_S} \hat{I}(0) = -\underbrace{\begin{bmatrix} 100 & 0 \\ 0 & 500 \end{bmatrix}}_{\hat{Z}_S} \hat{I}(0)$$

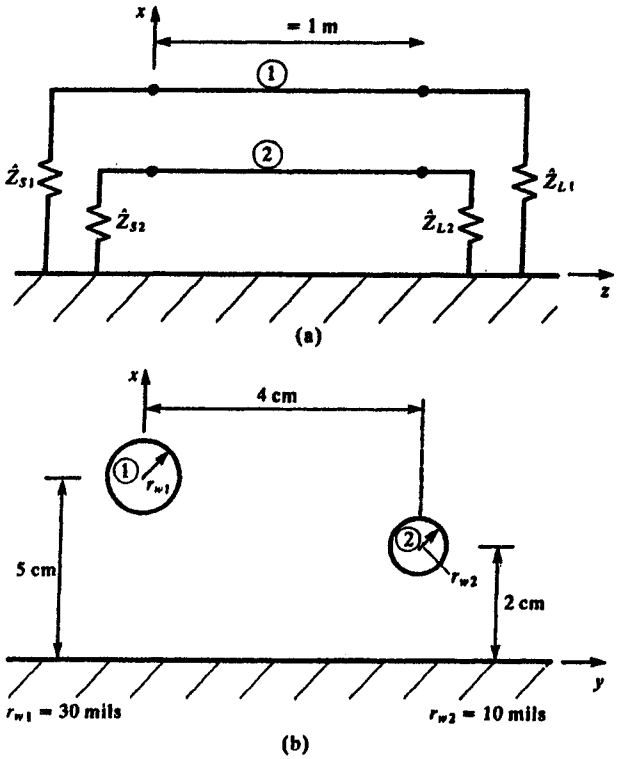

FIGURE 7.16 A three-conductor line consisting of two wires above a ground plane for illustration of computed results.

$$\hat{\mathbf{V}}(\mathscr{L}) = \underbrace{\begin{bmatrix} \hat{Z}_{L1} & 0 \\ 0 & \hat{Z}_{L2} \end{bmatrix}}_{\hat{\mathbf{Z}}_L} \hat{\mathbf{I}}(\mathscr{L}) = \underbrace{\begin{bmatrix} 500 & 0 \\ 0 & 1000 \end{bmatrix}}_{\hat{\mathbf{Z}}_L} \hat{\mathbf{I}}(\mathscr{L})$$

The first case has a 1 V/m uniform plane wave traveling parallel to the ground plane with the electric field perpendicular to the ground plane: $\theta_E = 90°$, $\theta_P = 90°$, $\phi_P = -90°$. The results of the code **INCIDENT.FOR** described in Appendix A at a frequency of 100 MHz are

$$I_1(0) = 4.637\,89E-4\underline{/-37.082°}\ \text{A},\quad I_1(\mathscr{L}) = 1.1502E-4\underline{/-156.86°}\ \text{A}$$
$$I_2(0) = 6.601\,77E-5\underline{/-24.279°}\ \text{A},\quad I_2(\mathscr{L}) = 3.0208E-6\underline{/70.154\,6°}\ \text{A}$$

These are identical to those of the **WIRE** program described in [H.1]. The next case has the 1 V/m uniform plane wave traveling in the $-x$ direction (perpendicular to the ground plane) with the electric field in the $+z$ direction

(parallel to the wires): $\theta_E = 0°$, $\theta_P = 0°$, $\phi_P = 0°$. The results of the code **INCIDENT.FOR** described in Appendix A at a frequency of 100 MHz are

$$I_1(0) = 5.3161E-4\underline{/-33.826°}\ \text{A},\quad I_1(\mathscr{L}) = 1.9875E-4\underline{/-6.817°}\ \text{A}$$
$$I_2(0) = 8.3918E-5\underline{/52.795°}\ \text{A},\quad I_2(\mathscr{L}) = 4.63388E-5\underline{/35.7719°}\ \text{A}$$

These are again identical to those of the **WIRE** program described in [H.1]. The frequency response for this case is plotted for wire #2 in Fig. 7.17. As before, these frequency-domain transfer functions can be used along with the **TIMEFREQ.FOR** program to compute the time-domain response for a plane wave having any waveshape.

7.3 TIME-DOMAIN SOLUTIONS

The time-domain solutions can be obtained with techniques analogous to those for no incident field as discussed in Chapter 5. Virtually all of those techniques can be used for the incident-field case. We essentially need to solve the time-domain MTL equations given in (7.18) and (7.19) or the form given in (7.20) and (7.21) for some arbitrary time variation of the incident field. We will choose to solve the forms in (7.18) and (7.19) which are in terms of the *total* voltages and currents. The following sections will concentrate on the solution for *lossless lines* although applications to the lossy-line case will be considered. Thus the equations to be solved are given in (7.18) and (7.19) with $\mathbf{R} = \mathbf{G} = \mathbf{0}$:

$$\frac{\partial}{\partial z}\mathbf{V}(z,t) + \mathbf{L}\frac{\partial}{\partial t}\mathbf{I}(z,t) = \mathbf{V}_F(z,t) \tag{7.137a}$$

$$\frac{\partial}{\partial z}\mathbf{I}(z,t) + \mathbf{C}\frac{\partial}{\partial t}\mathbf{V}(z,t) = \mathbf{I}_F(z,t) \tag{7.137b}$$

where

$$\mathbf{V}_F(z,t) = \frac{\partial}{\partial t}\begin{bmatrix} \vdots \\ \displaystyle\int_a^{a'} \vec{\mathscr{B}}^i \cdot \hat{a}_n\, dl \\ \vdots \end{bmatrix} \tag{7.138a}$$

$$= \begin{bmatrix} \vdots \\ \displaystyle -\frac{\partial}{\partial z}\int_a^{a'} \vec{\mathscr{E}}_t^i \cdot d\vec{l} + \{\mathscr{E}_z^i(i\text{-th conductor}, z, t) \\ \qquad - \mathscr{E}_z^i(\text{reference conductor}, z, t)\} \\ \vdots \end{bmatrix}$$

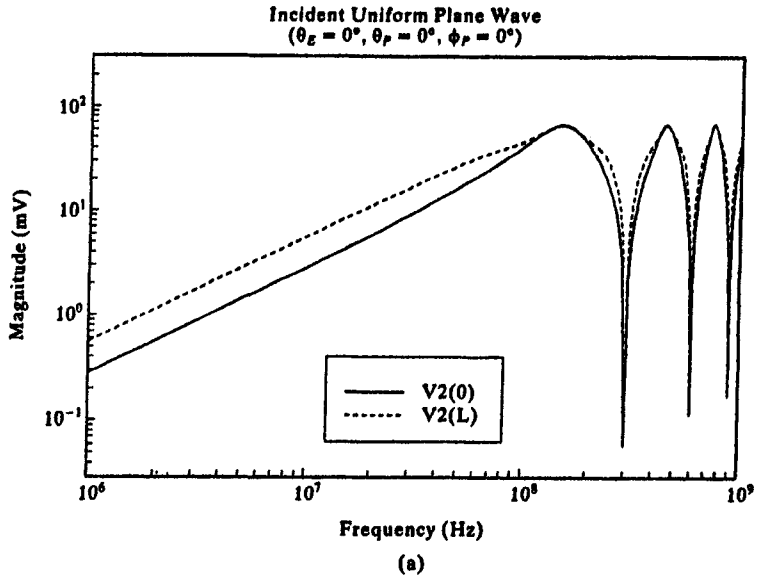

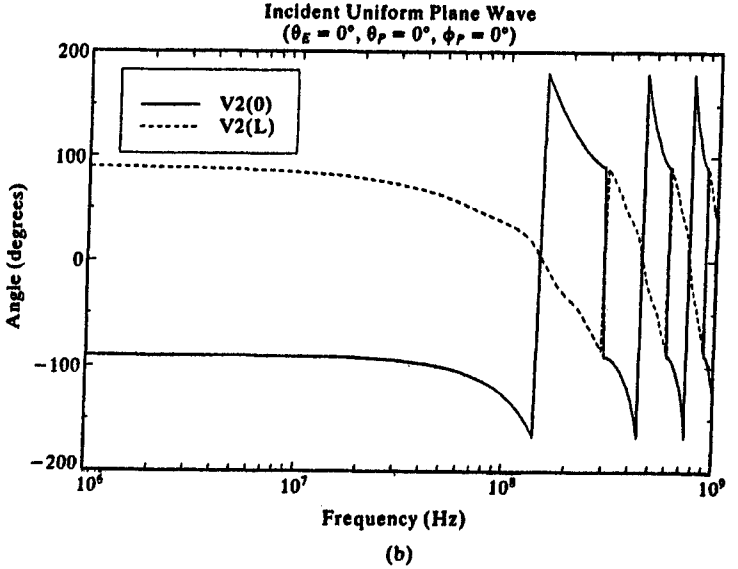

FIGURE 7.17 The computed frequency response for the line of Fig. 7.16: (a) magnitude, (b) phase. $\theta_E = 0$, $\theta_p = 0$, $\phi_p = 0$.

$$\mathbf{I}_F(z,t) = -\mathbf{C}\frac{\partial}{\partial t}\begin{bmatrix} \vdots \\ \int_a^{a'} \vec{\mathscr{E}}_t^i \cdot d\vec{l} \\ \vdots \end{bmatrix} \tag{7.138b}$$

We first concentrate on the solution for two-conductor lines. The solution for the multiconductor case will be obtained in terms of this solution by diagonalizing the MTL equations in the usual fashion.

7.3.1 Two-Conductor Lossless Lines

7.3.1.1 The General Solution via the Method of Characteristics The transmission-line equations for a two-conductor, lossless line become

$$\frac{\partial}{\partial z}V(z,t) + l\frac{\partial}{\partial t}I(z,t) = \frac{\partial}{\partial t}\mathscr{B}_N(z,t) \tag{7.139a}$$

$$= \mathscr{E}_L(z,t) - \frac{\partial}{\partial z}\mathscr{E}_T(z,t)$$

$$\frac{\partial}{\partial z}I(z,t) + c\frac{\partial}{\partial t}V(z,t) = -c\frac{\partial}{\partial t}\mathscr{E}_T(z,t) \tag{7.139b}$$

where

$$\mathscr{E}_L(z,t) = \mathscr{E}_z^i(d,z,t) - \mathscr{E}_z^i(0,z,t) \tag{7.140a}$$

$$\mathscr{E}_T(z,t) = \int_0^d \mathscr{E}_x^i(x,z,t)\,dx \tag{7.140b}$$

and the conductors lie in the x–z plane with the reference conductor located at $x = 0$ and the other conductor located at $x = d$ as illustrated in Fig. 7.8. The method of characteristics was used to obtain the time-domain solution in Chapter 5 for the transmission-line equations that did not have forcing functions on the right-hand side. Here we extend that method to solve (7.139). A similar derivation was given in [17]. The total differentials are

$$dV = \frac{\partial V}{\partial z}dz + \frac{\partial V}{\partial t}dt \tag{7.141a}$$

$$dI = \frac{\partial I}{\partial z}dz + \frac{\partial I}{\partial t}dt \tag{7.141b}$$

$$d\mathscr{E}_T = \frac{\partial \mathscr{E}_T}{\partial z}dz + \frac{\partial \mathscr{E}_T}{\partial t}dt \tag{7.141c}$$

$$d\mathscr{E}_L = \frac{\partial \mathscr{E}_L}{\partial z}\,dz + \frac{\partial \mathscr{E}_L}{\partial t}\,dt \tag{7.141d}$$

Substituting the transmission-line equations given in (7.139) into (7.141a) and (7.141b) yields

$$dV = \left(-l\frac{\partial I}{\partial t} + \mathscr{E}_L - \frac{\partial \mathscr{E}_T}{\partial z}\right)dz + \frac{\partial V}{\partial t}\,dt \tag{7.142a}$$

$$dI = \left(-c\frac{\partial V}{\partial t} - c\frac{\partial \mathscr{E}_T}{\partial t}\right)dz + \frac{\partial I}{\partial t}\,dt \tag{7.142b}$$

The characteristic curves are drawn as shown in Fig. 5.7. Along the *forward characteristic*, $dz = v\,dt$ where the velocity of propagation along the line is $v = 1/\sqrt{lc}$. Substituting this into (7.142) and defining the characteristic impedance of the line as $Z_C = vl = 1/vc$ yields

$$dV = \left(-Z_C\frac{\partial I}{\partial t} + v\mathscr{E}_L - v\frac{\partial \mathscr{E}_T}{\partial z} + \frac{\partial V}{\partial t}\right)dt \tag{7.143a}$$

$$dI = \left(-\frac{1}{Z_C}\frac{\partial V}{\partial t} - \frac{1}{Z_C}\frac{\partial \mathscr{E}_T}{\partial t} + \frac{\partial I}{\partial t}\right)dt \tag{7.143b}$$

Adding these gives

$$dV + Z_C\,dI = \left(v\mathscr{E}_L - v\frac{\partial \mathscr{E}_T}{\partial z} - \frac{\partial \mathscr{E}_T}{\partial t}\right)dt \tag{7.144}$$

Substituting (7.141c) yields

$$dV + Z_C\,dI = \mathscr{E}_L\,dz - d\mathscr{E}_T \tag{7.145}$$

Rearranging and integrating along the forward characteristic from $z = 0$ to $z = \mathscr{L}$ gives

$$\int_0^{\mathscr{L}} \left(\frac{dV}{dz} + Z_C\frac{dI}{dz} + \frac{d\mathscr{E}_T}{dz}\right)dz = \int_0^{\mathscr{L}} \mathscr{E}_L\,dz \tag{7.146}$$

or

$$V(\mathscr{L}, t) + Z_C I(\mathscr{L}, t) = V(0, t - T) + Z_C I(0, t - T) + \mathscr{E}_T(0, t - T) - \mathscr{E}_T(\mathscr{L}, t) + \int_0^{\mathscr{L}} \mathscr{E}_L\left(z, t - T + \frac{z}{v}\right)dz \tag{7.147}$$

where the one-way line delay is $T = \mathscr{L}/v$. The result in the integral is due to the fact that along the forward characteristic, t and z are related as $t = z/v + C^+$.

Similarly, along the *backward characteristic*, $dz = -v\,dt$. Substituting this into (7.142) yields

$$dV = \left(Z_C \frac{\partial I}{\partial t} - v\mathscr{E}_L + v\frac{\partial \mathscr{E}_T}{\partial z} + \frac{\partial V}{\partial t}\right) dt \tag{7.148a}$$

$$dI = \left(\frac{1}{Z_C}\frac{\partial V}{\partial t} + \frac{1}{Z_C}\frac{\partial \mathscr{E}_T}{\partial t} + \frac{\partial I}{\partial t}\right) dt \tag{7.148b}$$

Subtracting these gives

$$dV - Z_C\,dI = \left(-v\mathscr{E}_L + v\frac{\partial \mathscr{E}_T}{\partial z} - \frac{\partial \mathscr{E}_T}{\partial t}\right) dt \tag{7.149}$$

Substituting (7.141c) yields

$$dV - Z_C\,dI = \mathscr{E}_L\,dz - d\mathscr{E}_T \tag{7.150}$$

Rearranging and integrating along the forward characteristic from $z = 0$ to $z = \mathscr{L}$ gives

$$\int_0^{\mathscr{L}} \left(\frac{dV}{dz} - Z_C\frac{dI}{dz} + \frac{d\mathscr{E}_T}{dz}\right) dz = \int_0^{\mathscr{L}} \mathscr{E}_L\,dz \tag{7.151}$$

or

$$V(0,t) - Z_C I(0,t) = V(\mathscr{L}, t-T) - Z_C I(\mathscr{L}, t-T) + \mathscr{E}_T(\mathscr{L}, t-T) \tag{7.152}$$
$$- \mathscr{E}_T(0,t) - \int_0^{\mathscr{L}} \mathscr{E}_L\left(z, t - \frac{z}{v}\right) dz$$

The result in the integral is due to the fact that along the backward characteristic, t and z are related as $t = -z/v + C^-$.

The results in (7.147) and (7.152) relate the voltages and currents at one end of the line to those at the other end delayed by the line one-way delay, T, as well as various values of the transverse and longitudinal incident electric fields. These are similar to the results derived in Chapter 5 for no incident field and will again allow us to construct a SPICE model of the line.

7.3.1.2 The General Solution via the Frequency Domain As before, a simple method of determining the time-domain solution is to transform the frequency-domain solution. The frequency-domain chain parameter matrix for a lossless line excited by an incident field is

$$\hat{V}(\mathscr{L}) = \hat{\phi}_{11}(\mathscr{L})\hat{V}(0) + \hat{\phi}_{12}(\mathscr{L})\hat{I}(0) + \hat{V}_{FT}(\mathscr{L}) \tag{7.153a}$$

$$\hat{I}(\mathscr{L}) = \hat{\phi}_{21}(\mathscr{L})\hat{V}(0) + \hat{\phi}_{22}(\mathscr{L})\hat{I}(0) + \hat{I}_{FT}(\mathscr{L}) \tag{7.153b}$$

where the scalar chain parameters are given by

$$\hat{\phi}_{11}(\mathscr{L}) = \cos(\beta\mathscr{L}) \tag{7.154a}$$

$$\hat{\phi}_{12}(\mathscr{L}) = -jZ_C^{-1}\sin(\beta\mathscr{L}) \tag{7.154b}$$

$$\hat{\phi}_{21}(\mathscr{L}) = -jZ_C^{-1}\sin(\beta\mathscr{L}) \tag{7.154c}$$

$$\hat{\phi}_{22}(\mathscr{L}) = \cos(\beta\mathscr{L}) \tag{7.154d}$$

Moving the forcing functions produced by the incident field to the left-hand side of (7.153) gives

$$\hat{V}'(\mathscr{L}) = [\hat{V}(\mathscr{L}) - \hat{V}_{FT}(\mathscr{L})] = \hat{\phi}_{11}(\mathscr{L})\hat{V}(0) + \hat{\phi}_{12}(\mathscr{L})\hat{I}(0) \tag{7.155a}$$

$$\hat{I}'(\mathscr{L}) = [\hat{I}(\mathscr{L}) - \hat{I}_{FT}(\mathscr{L})] = \hat{\phi}_{21}(\mathscr{L})\hat{V}(0) + \hat{\phi}_{22}(\mathscr{L})\hat{I}(0) \tag{7.155b}$$

If we take the inverse Fourier transform of this result, we see that *the incident-field-excited line shown in Fig.* 7.18(*a*) *can be characterized as the cascade of the unexcited line and independent sources representing the effects of the incident field,* $V_{FT}(\mathscr{L}, t)$ *and* $I_{FT}(\mathscr{L}, t)$, *as shown in Fig.* 7.18(*b*) *where*

$$\hat{V}_{FT}(\mathscr{L}) \Leftrightarrow V_{FT}(\mathscr{L}, t) \tag{7.156a}$$

$$\hat{I}_{FT}(\mathscr{L}) \Leftrightarrow I_{FT}(\mathscr{L}, t) \tag{7.156b}$$

Therefore, the basic problem is to determine the time-domain representations of the incident field forcing functions as in (7.156).

The method of characteristics was used previously to derive relations between the voltages and currents at one end of the line in terms of the voltages and currents at the other end delayed by the one-way time delay and the longitudinal and transverse components of the incident electric field and are given in (7.147) and (7.152). We now prove, by transforming the above frequency-domain result to the time domain, that the correct derivation was obtained. Substituting the chain parameters given in (7.154) into (7.153) yields

$$\hat{V}(\mathscr{L}) = \left(\frac{e^{j\beta\mathscr{L}} + e^{-j\beta\mathscr{L}}}{2}\right)\hat{V}(0) - \left(\frac{e^{j\beta\mathscr{L}} - e^{-j\beta\mathscr{L}}}{2}\right)Z_C\hat{I}(0) + \hat{V}_{FT}(\mathscr{L}) \tag{7.157a}$$

$$Z_C\hat{I}(\mathscr{L}) = -\left(\frac{e^{j\beta\mathscr{L}} - e^{-j\beta\mathscr{L}}}{2}\right)\hat{V}(0) + \left(\frac{e^{j\beta\mathscr{L}} + e^{-j\beta\mathscr{L}}}{2}\right)Z_C\hat{I}(0) + Z_C\hat{I}_{FT}(\mathscr{L}) \tag{7.157b}$$

(We have multiplied the second equation by the characteristic impedance, Z_C,

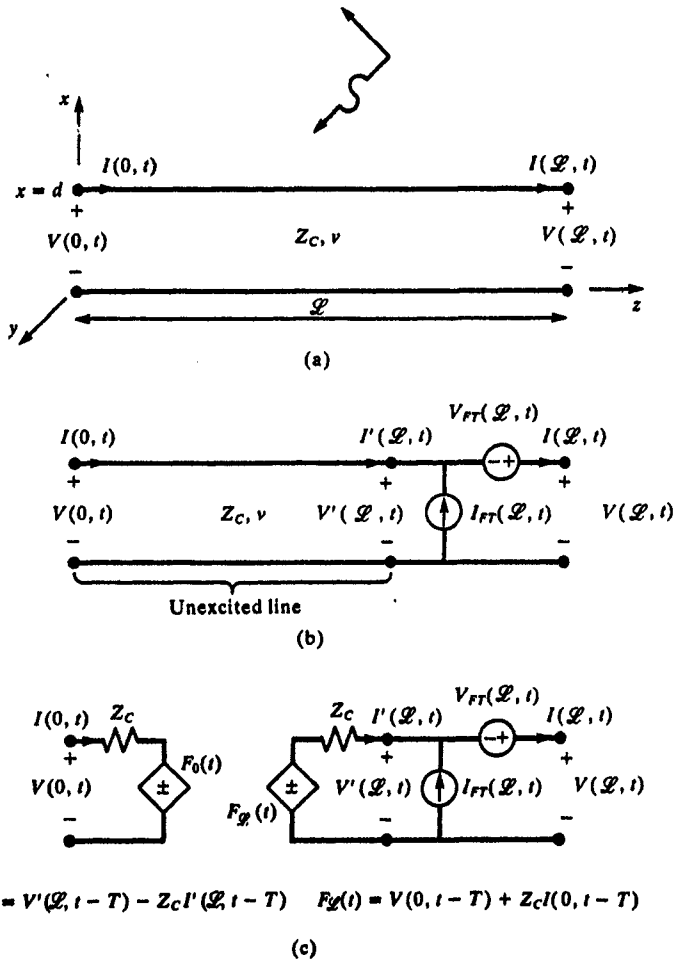

FIGURE 7.18 A generalized method of characteristics model of a two-conductor line with incident field illumination: (a) the line, (b) lumping the effects of the incident field as sources, and (c) representing the unexcited portion with time-delay-controlled sources.

in order to simplify the following.) Adding and subtracting these gives

$$\hat{V}(0) - Z_C\hat{I}(0) = e^{-j\beta\mathscr{L}}[\hat{V}(\mathscr{L}) - Z_C\hat{I}(\mathscr{L})] - e^{-j\beta\mathscr{L}}[\hat{V}_{FT}(\mathscr{L}) - Z_C\hat{I}_{FT}(\mathscr{L})] \tag{7.158a}$$

$$\hat{V}(\mathscr{L}) + Z_C\hat{I}(\mathscr{L}) = e^{-j\beta\mathscr{L}}[\hat{V}(0) + Z_C\hat{I}(0)] + [\hat{V}_{FT}(\mathscr{L}) + Z_C\hat{I}_{FT}(\mathscr{L})] \tag{7.158b}$$

Recognizing the basic time delay:

$$e^{\pm j\beta\mathscr{L}}\hat{F}(\omega) \Leftrightarrow f(t \pm T) \tag{7.159}$$

where

$$\beta = \frac{\omega}{v} \tag{7.160a}$$

and the line one-way delay is again

$$T = \frac{\mathscr{L}}{v} \tag{7.160b}$$

these transform to the time domain as

$$V(0,t) - Z_C I(0,t) = [V(\mathscr{L}, t-T) - Z_C I(\mathscr{L}, t-T)] - [V_{FT}(\mathscr{L}, t-T) - Z_C I_{FT}(\mathscr{L}, t-T)] \tag{7.161a}$$

$$V(\mathscr{L},t) + Z_C I(\mathscr{L},t) = [V(0, t-T) + Z_C I(0, t-T)] + [V_{FT}(\mathscr{L}, t) + Z_C I_{FT}(\mathscr{L}, t)] \tag{7.161b}$$

The equivalence of these results to those obtained with the method of characteristics and given in (7.147) and (7.152) can be demonstrated by substituting the frequency-domain expressions for $\hat{V}_{FT}(\mathscr{L})$ given in (7.84) and $\hat{I}_{FT}(\mathscr{L})$ given in (7.85) into (7.158) to yield

$$\hat{V}_{FT}(\mathscr{L}) + Z_C \hat{I}_{FT}(\mathscr{L}) = \int_0^{\mathscr{L}} e^{-j\beta(\mathscr{L}-z)} \hat{E}_L(z)\, dz - \hat{E}_T(\mathscr{L}) + e^{-j\beta\mathscr{L}} \hat{E}_T(0) \tag{7.162a}$$

$$\Leftrightarrow \int_0^{\mathscr{L}} \mathscr{E}_L\left(z, t - T + \frac{z}{v}\right) dz - \mathscr{E}_T(\mathscr{L}, t) + \mathscr{E}_T(0, t-T)$$

$$-e^{-j\beta\mathscr{L}}[\hat{V}_{FT}(\mathscr{L}) - Z_C \hat{I}_{FT}(\mathscr{L})] = -\int_0^{\mathscr{L}} e^{-j\beta z} \hat{E}_L(z)\, dz + e^{-j\beta\mathscr{L}} \hat{E}_T(\mathscr{L}) + \hat{E}_T(0) \tag{7.162b}$$

$$\Leftrightarrow -\int_0^{\mathscr{L}} \mathscr{E}_L\left(z, t - \frac{z}{v}\right) dz + \mathscr{E}_T(\mathscr{L}, t-T) - \mathscr{E}_T(0,t)$$

Comparing these to (7.147) and (7.152) we observe the equivalence between the two results.

We next derive an explicit result for the time-domain voltages at the ends of the line for resistive loads, $\hat{V}(0) = -R_S \hat{I}(0)$ and $\hat{V}(\mathscr{L}) = R_L \hat{I}(\mathscr{L})$. Substituting these terminal constraints into (7.158) yields the terminal voltages as

$$\hat{V}(0) = \frac{e^{-j\beta\mathscr{L}}(\Gamma_L - 1)\hat{V}_{FT}(\mathscr{L}) + e^{-j\beta\mathscr{L}}(\Gamma_L + 1)Z_C\hat{I}_{FT}(\mathscr{L})}{[1 - \Gamma_S\Gamma_L e^{-j2\beta\mathscr{L}}]} \frac{R_S}{R_S + Z_C} \tag{7.163a}$$

$$\hat{V}(\mathscr{L}) = \frac{(1 - \Gamma_S e^{-j2\beta\mathscr{L}})\hat{V}_{FT}(\mathscr{L}) + (1 + \Gamma_S e^{-j2\beta\mathscr{L}})Z_C\hat{I}_{FT}(\mathscr{L})}{[1 - \Gamma_S\Gamma_L e^{-j2\beta\mathscr{L}}]} \frac{R_L}{R_L + Z_C} \tag{7.163b}$$

where the reflection coefficients are given by

$$\Gamma_S = \frac{R_S - Z_C}{R_S + Z_C} \tag{7.164a}$$

$$\Gamma_L = \frac{R_L - Z_C}{R_L + Z_C} \tag{7.164b}$$

The time-domain solution is obtained from this result by recognizing the basic result given in (7.159) as

$$V(0, t) - \Gamma_S\Gamma_L V(0, t - 2T) = [(\Gamma_L - 1)V_{FT}(\mathscr{L}, t - T) + (\Gamma_L + 1)Z_C I_{FT}(\mathscr{L}, t - T)] \frac{R_S}{R_S + Z_C} \tag{7.165a}$$

$$V(0, t) - \Gamma_S\Gamma_L V(0, t - 2T) = [V_{FT}(\mathscr{L}, t) - \Gamma_S V_{FT}(\mathscr{L}, t - 2T) + Z_C I_{FT}(\mathscr{L}, t) + \Gamma_S Z_C I_{FT}(\mathscr{L}, t - 2T)] \frac{R_S}{R_L + Z_C} \tag{7.165b}$$

These are *implicit* relations in that the value of a solution variable, $V(0, t)$, depends on the value two one-way line delays earlier, $V(0, t - 2T)$. An explicit recursion relation can be obtained with the *time-shift* or *difference operator*, D, as was done in Chapter 6:

$$D^{\pm k} f(t) = f(t \pm kT) \tag{7.166}$$

Thus the results in (7.165) become,

$$V(0, t) = \frac{(\Gamma_L - 1)DV_{FT}(\mathscr{L}, t) + (\Gamma_L + 1)Z_C DI_{FT}(\mathscr{L}, t)}{[D^2 - \alpha]} \frac{R_S}{R_S + Z_C} \tag{7.167a}$$

$$= \frac{\Gamma_L D[V_{FT}(\mathscr{L}, t) + Z_C I_{FT}(\mathscr{L}, t)] - D[V_{FT}(\mathscr{L}, t) - Z_C I_{FT}(\mathscr{L}, t)]}{[D^2 - \alpha]} \frac{R_S}{R_S + Z_C}$$

$$V(\mathscr{L}, t) = \frac{(D^2 - \Gamma_S)V_{FT}(\mathscr{L}, t) + (D^2 + \Gamma_S)Z_C I_{FT}(\mathscr{L}, t)}{[D^2 - \alpha]} \frac{R_L}{R_L + Z_C} \tag{7.167b}$$

$$= \frac{D^2[V_{FT}(\mathscr{L}, t) + Z_C I_{FT}(\mathscr{L}, t)] - \Gamma_S[V_{FT}(\mathscr{L}, t) - Z_C I_{FT}(\mathscr{L}, t)]}{[D^2 - \alpha]} \frac{R_L}{R_L + Z_C}$$

where

$$\alpha = \Gamma_S \Gamma_L \tag{7.168}$$

Carrying out the long division and substituting (7.166) gives

$$\begin{aligned} V(0,t) = \frac{R_S}{R_S + Z_C} \{ & (\Gamma_L - 1)[V_{FT}(\mathscr{L}, t-T) + \alpha V_{FT}(\mathscr{L}, t-3T) \\ & + \alpha^2 V_{FT}(\mathscr{L}, t-5T) + \cdots] + (\Gamma_L + 1) Z_C [I_{FT}(\mathscr{L}, t-T) \\ & + \alpha I_{FT}(\mathscr{L}, t-3T) + \alpha^2 I_{FT}(\mathscr{L}, t-5T) + \cdots] \} \end{aligned} \tag{7.169a}$$

$$\begin{aligned} V(\mathscr{L}, t) = \frac{R_L}{R_L + Z_C} \{ & [V_{FT}(\mathscr{L}, t) + \alpha V_{FT}(\mathscr{L}, t-2T) \\ & + \alpha^2 V_{FT}(\mathscr{L}, t-4T) + \cdots] + Z_C [I_{FT}(\mathscr{L}, t) \\ & + \alpha I_{FT}(\mathscr{L}, t-2T) + \alpha^2 I_{FT}(\mathscr{L}, t-4T) + \cdots] \\ & - \Gamma_S [V_{FT}(\mathscr{L}, t-2T) + \alpha V_{FT}(\mathscr{L}, t-4T) \\ & \times \alpha^2 V_{FT}(\mathscr{L}, t-6T) + \cdots] \\ & + \Gamma_S Z_C [I_{FT}(\mathscr{L}, t-2T) \\ & + \alpha I_{FT}(\mathscr{L}, t-4T) + \alpha^2 I_{FT}(\mathscr{L}, t-6T) + \cdots] \} \end{aligned} \tag{7.169b}$$

Thus the terminal voltages are weighted sums of the functions produced by the incident field, $\hat{V}_{FT}(\mathscr{L}) \Leftrightarrow V_{FT}(\mathscr{L}, t)$ and $\hat{I}_{FT}(\mathscr{L}) \Leftrightarrow I_{FT}(\mathscr{L}, t)$, delayed in time by multiples of the line one-way delay, T. Thus the basic problem here is again to determine the frequency-domain to time-domain transformations of the functions representing the effect of the incident field given in (7.156). Other series expansions for the time-domain solution are given in [5, 18].

7.3.1.3 Uniform Plane-Wave Excitation of the Line Although the above results are valid for any time form of the incident-field excitation, a useful form is that of a uniform plane wave. Consider a two-conductor line shown in Fig. 7.8 with line conductors located in the x–z plane at $x = 0$, $y = 0$ and $x = d$, $y = 0$ and extending from $z = 0$ to $z = \mathscr{L}$. The frequency-domain forcing functions are given in (7.84) and (7.85). We consider a uniform plane wave incident on the line whose frequency-domain representation is

$$\hat{\vec{E}}^i(x, y, z, \omega) = \hat{E}_0(\omega)(e_x \hat{a}_x + e_y \hat{a}_y + e_z \hat{a}_z) e^{-j\beta_x x} e^{-j\beta_y y} e^{-j\beta_z z} \tag{7.170}$$

where the components of the incident electric field vector along the x, y, and z axes of the rectangular coordinate system describing the line are

$$\left.\begin{aligned} e_x &= \sin\theta_E \sin\theta_p \\ e_y &= -\sin\theta_E \cos\theta_p \cos\phi_p - \cos\theta_E \sin\phi_p \\ e_z &= -\sin\theta_E \cos\theta_p \sin\phi_p + \cos\theta_E \cos\phi_p \end{aligned}\right\} \tag{7.171a}$$

The angles are with reference to Fig. 7.6. The components of the phase constant along those coordinate axes are

$$\left.\begin{aligned}\beta_x &= -\beta\cos\theta_p\\ \beta_y &= -\beta\sin\theta_p\cos\phi_p\\ \beta_z &= -\beta\sin\theta_p\sin\phi_p\end{aligned}\right\} \tag{7.171b}$$

In the time domain, (7.170) translates to [A.1]

$$\vec{\mathscr{E}}^i(x,y,z,t) = (e_x\hat{a}_x + e_y\hat{a}_y + e_z\hat{a}_z)\mathscr{E}_o\left(t - \frac{x}{v_x} - \frac{y}{v_y} - \frac{z}{v_z}\right) \tag{7.172}$$

The time form of the electric field is denoted by $\mathscr{E}_o(t)$ where $\mathscr{E}_o(t) \Leftrightarrow \hat{E}_o(\omega)$, and the velocities of propagation along the axes are denoted by

$$\left.\begin{aligned}v_x &= \frac{\omega}{\beta_x} = -\frac{v}{\cos\theta_p}\\ v_y &= \frac{\omega}{\beta_y} = -\frac{v}{\sin\theta_p\cos\phi_p}\\ v_z &= \frac{\omega}{\beta_z} = -\frac{v}{\sin\theta_p\sin\phi_p}\end{aligned}\right\} \tag{7.173}$$

The frequency-domain forcing functions, given in (7.84) and (7.85), become

$$\begin{aligned}\hat{V}_{FT}(\mathscr{L}) = \left[\frac{\sin(\beta_x d/2)}{\beta_x d/2}\right]\frac{d}{2}\hat{E}_o(\omega)e^{-j\beta_x d/2} \\ \times\left\{\left[e_x - e_z\left(\frac{\beta_x}{\beta+\beta_z}\right)\right](e^{j\beta\mathscr{L}} - e^{-j\beta_z\mathscr{L}})\right. \\ \left. + \left[e_x + e_z\left(\frac{\beta_x}{\beta-\beta_z}\right)\right](e^{-j\beta\mathscr{L}} - e^{-j\beta_z\mathscr{L}})\right\}\end{aligned} \tag{7.174}$$

$$\begin{aligned}\hat{I}_{FT}(\mathscr{L}) = \left[\frac{\sin(\beta_x d/2)}{\beta_x d/2}\right]\frac{d}{2Z_C}\hat{E}_o(\omega)e^{-j\beta_x d/2} \\ \times\left\{\left[-e_x + e_z\left(\frac{\beta_x}{\beta+\beta_z}\right)\right](e^{j\beta\mathscr{L}} - e^{-j\beta_z\mathscr{L}})\right. \\ \left. + \left[e_x + e_z\left(\frac{\beta_x}{\beta-\beta_z}\right)\right](e^{-j\beta\mathscr{L}} - e^{-j\beta_z\mathscr{L}})\right\}\end{aligned} \tag{7.175}$$

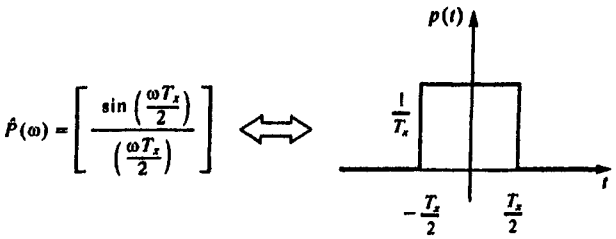

FIGURE 7.19 The pulse function representing the effect of propagation in the cross-sectional plane.

The time-domain forms can be obtained by first noting that

$$\hat{P}(\omega) = \left[\frac{\sin(\beta_x d/2)}{\beta_x d/2}\right] \tag{7.176}$$

is equivalent, in the time domain, to the pulse function [A.2, A.3]

$$p(t) = \begin{cases} 0 & t < -\dfrac{T_x}{2} \\ \dfrac{1}{T_x} & -\dfrac{T_x}{2} < t < \dfrac{T_x}{2} \\ 0 & t > \dfrac{T_x}{2} \end{cases} \tag{7.177a}$$

where

$$T_x = \frac{d}{v_x} \tag{7.177b}$$

is the transit delay from one conductor to the other as illustrated in Fig. 7.19. Therefore the time-domain forcing functions, $V_{FT}(\mathscr{L}, t)$ and $I_{FT}(\mathscr{L}, t)$ given in (7.174) and (7.175), are the convolution of the pulse function and the functions

$$\begin{aligned} V(t) = \frac{d}{2}\Bigg\{ & e_x\left[\mathscr{E}_0\left(t + T - \frac{T_x}{2}\right) + \mathscr{E}_0\left(t - T - \frac{T_x}{2}\right) - 2\mathscr{E}_0\left(t - T_z - \frac{T_x}{2}\right)\right] \\ & - e_z\left(\frac{\mathscr{L}}{v_x}\right)\left[\frac{\mathscr{E}_0\left(t + T - \frac{T_x}{2}\right) - \mathscr{E}_0\left(t - T_z - \frac{T_x}{2}\right)}{(T_z + T)}\right] \\ & - e_z\left(\frac{\mathscr{L}}{v_x}\right)\left[\frac{\mathscr{E}_0\left(t - T - \frac{T_x}{2}\right) - \mathscr{E}_0\left(t - T_z - \frac{T_x}{2}\right)}{(T_z - T)}\right]\Bigg\} \end{aligned} \tag{7.178}$$

$$I(t) = \frac{d}{2Z_C}\left\{-e_x\left[\mathscr{E}_0\left(t + T - \frac{T_x}{2}\right) - \mathscr{E}_0\left(t - T - \frac{T_x}{2}\right)\right]\right. \tag{7.179}$$
$$+ e_z\left(\frac{\mathscr{L}}{v_x}\right)\left[\frac{\mathscr{E}_0\left(t + T - \frac{T_x}{2}\right) - \mathscr{E}_0\left(t - T_z - \frac{T_x}{2}\right)}{(T_z + T)}\right]$$
$$\left. - e_z\left(\frac{\mathscr{L}}{v_x}\right)\left[\frac{\mathscr{E}_0\left(t - T - \frac{T_x}{2}\right) - \mathscr{E}_0\left(t - T_z - \frac{T_x}{2}\right)}{(T_z - T)}\right]\right\}$$

as

$$V_{FT}(\mathscr{L}, t) = \int_{-\infty}^{\infty} V(\tau)p(t - \tau)\,d\tau \tag{7.180}$$
$$= V(t) * p(t)$$

$$I_{FT}(\mathscr{L}, t) = \int_{-\infty}^{\infty} I(\tau)p(t - \tau)\,d\tau \tag{7.181}$$
$$= I(t) * p(t)$$

where the transit time along the line of the z component of the wave propagation vector is

$$T_z = \frac{\mathscr{L}}{v_z} \tag{7.182}$$

and the transit time of the waves on the line is

$$T = \frac{\mathscr{L}}{v} \tag{7.183}$$

The transit time of the wave in the cross-sectional plane:

$$T_x = \frac{d}{v_x} \tag{7.184}$$

is normally small because of the requirement that the line cross-sectional dimensions be electrically small in order for the transmission-line model to be valid, so we can usually disregard this time delay. When $v_z = \pm v$ as when the wave is traveling solely in the $\pm z$ direction, one term in (7.178) and (7.179) appears to be undefined. However that term also contains $v_x = \infty$ so the term becomes zero.

Observe that if the line cross section is sufficiently small over the spectrum of $\hat{E}_o(\omega)$ then the pulse function, $p(t)$, approximates an impulse function:

$$p(t) \cong \delta(t) \qquad \text{small } T_x \tag{7.185}$$

and the forcing functions are approximated by

$$V_{FT}(\mathscr{L}, t) \cong V(t) \tag{7.186}$$

$$I_{FT}(\mathscr{L}, t) \cong I(t) \tag{7.187}$$

If the propagation vector has no component in the x direction, $\beta_x = 0$ or $v_x = \infty$, then (7.186) and (7.187) are *exact*. Again, in order for the transmission-line model to be valid, the line cross-sectional dimensions must be electrically small at all frequencies of interest. Thus, as a practical matter, we may assume that (7.186) and (7.187) are valid and may also omit the cross-sectional time delay, $T_x = d/v_x$, from the functions in (7.178) and (7.179).

In the case of a conductor located at a height h above an infinite ground plane as illustrated in Fig. 7.10, the above functions are easily modified. The *total* incident electric field (the incident field plus the field reflected from the ground plane) is given in the frequency domain in (7.112). The frequency-domain forcing functions given in (7.84) and (7.85) depend on the z and x components of the electric field. Substituting (7.112) ($x = h$ and $y = 0$) gives

$$\left[\hat{E}_z^{\text{total}}(h, z) - \underbrace{\hat{E}_z^{\text{total}}(0, z)}_{0}\right] = \left[-j2\beta_x h \frac{\sin(\beta_x h)}{\beta_x h)}\right]\hat{E}_o(\omega)e_z e^{-j\beta_z z} \tag{7.188a}$$

This compares to the case with no ground plane:

$$[\hat{E}_z^i(d, z) - \hat{E}_z^i(0, z)] = \left[-j2\beta_x \frac{d}{2}\frac{\sin(\beta_x d/2)}{\beta_x d/2} e^{-j\beta_x d/2}\right]\hat{E}_o(\omega)e_z e^{-j\beta_z z} \tag{7.188b}$$

Similarly,

$$\int_0^h \hat{E}_x^{\text{total}}\, dx = 2h\left[\frac{\sin(\beta_x h)}{\beta_x h}\right]\hat{E}_o(\omega)e_x e^{-j\beta_z z} \tag{7.189a}$$

This compares to the case with no ground plane:

$$\int_0^d \hat{E}_x^i\, dx = 2\left(\frac{d}{2}\right)\left[\frac{\sin(\beta_x d/2)}{\beta_x d/2} e^{-j\beta_x d/2}\right]\hat{E}_o(\omega)e_x e^{-j\beta_z z} \tag{7.189b}$$

Therefore, to convert the previous frequency-domain results to the case of a

ground plane, we simply remove the factor $e^{-j\beta_x d/2}$ and replace $d/2 \Leftrightarrow h$ in those results. The frequency-domain forcing functions, given in (7.84) and (7.85), become

$$\hat{V}_{FT}(\mathscr{L}) = h\hat{E}_o(\omega)\left[\frac{\sin(\beta_x h)}{\beta_x h}\right]\left\{\left[e_x - e_z\left(\frac{\beta_x}{\beta + \beta_x}\right)\right](e^{j\beta\mathscr{L}} - e^{-j\beta_z\mathscr{L}}) + \left[e_x + e_z\left(\frac{\beta_x}{\beta - \beta_x}\right)\right](e^{-j\beta\mathscr{L}} - e^{-j\beta_z\mathscr{L}})\right\} \quad (7.190)$$

$$\hat{I}_{FT}(\mathscr{L}) = \frac{h}{Z_C}\hat{E}_o(\omega)\left[\frac{\sin(\beta_x h)}{\beta_x h}\right]\left\{\left[-e_x + e_z\left(\frac{\beta_x}{\beta + \beta_x}\right)\right](e^{j\beta\mathscr{L}} - e^{-j\beta_z\mathscr{L}}) + \left[e_x + e_z\left(\frac{\beta_x}{\beta - \beta_x}\right)\right](e^{-j\beta\mathscr{L}} - e^{-j\beta_z\mathscr{L}})\right\} \quad (7.191)$$

Therefore the time-domain forcing functions are again given by the convolutions in (7.180) and (7.181) with $T_x/2$ removed and the pulse function, $p(t)$, has $d/2$ replaced with h: $d/2 \Leftrightarrow$ h.

The explicit, time-domain series solution given for resistive loads in (7.169) can be written in a more compact form for uniform plane-wave excitation as

$$V(0, t) = \left(\frac{R_S}{R_S + Z_C}\right)p(t) \quad (7.192a)$$
$$* \{\Gamma_L[M^+(t - T) + \alpha M^+(t - 3T) + \alpha^2 M^+(t - 5T) + \cdots] - [M^-(t - T) + \alpha M^-(t - 3T) + \alpha^2 M^-(t - 5T) + \cdots]\}$$

$$V(\mathscr{L}, t) = \left(\frac{R_L}{R_L + Z_C}\right)p(t) \quad (7.192b)$$
$$* \{[M^+(t) + \alpha M^+(t - 2T) + \alpha^2 M^+(t - 4T) + \cdots] - \Gamma_S[M^-(t - 2T) + \alpha M^-(t - 4T) + \alpha^2 M^-(t - 6T) + \cdots]\}$$

where

$$M^+(t) = V(t) + Z_C I(t) \quad (7.193a)$$
$$= A\left\{e_x\left(\frac{1}{v_z} - \frac{1}{v}\right) - e_z\left(\frac{1}{v_x}\right)\right\}\left[\frac{\mathscr{E}_o\left(t - T - \frac{T_x}{2}\right) - \mathscr{E}_o\left(t - T_z - \frac{T_x}{2}\right)}{T_z - T}\right]$$
$$\cong A\left\{e_x\left(\frac{1}{v_z} - \frac{1}{v}\right) - e_z\left(\frac{1}{v_x}\right)\right\}\left[\frac{\mathscr{E}_o(t - T) - \mathscr{E}_o(t - T_z)}{T_z - T}\right]$$

$$M^{-}(t) = V(t) - Z_C I(t) \tag{7.193b}$$

$$= A\left\{e_x\left(\frac{1}{v_z} + \frac{1}{v}\right) - e_z\left(\frac{1}{v_x}\right)\right\}\left[\frac{\mathscr{E}_0\left(t + T - \frac{T_x}{2}\right) - \mathscr{E}_0\left(t - T_z - \frac{T_x}{2}\right)}{T_z + T}\right]$$

$$\cong A\left\{e_x\left(\frac{1}{v_z} + \frac{1}{v}\right) - e_z\left(\frac{1}{v_x}\right)\right\}\left[\frac{\mathscr{E}_0(t + T) - \mathscr{E}_0(t - T_z)}{T_z + T}\right]$$

and the loop area of the line is denoted by

$$A = d\mathscr{L} \tag{7.193c}$$

In the case of a ground plane, replace $d \Leftrightarrow 2h$ in $M^{\pm}(t)$ and remove $T_x/2$.

*7.3.1.4 **Electrically Short Lines*** Simple frequency-domain results were obtained in Section 7.2.5.4 for a line that is electrically very short, i.e., $\mathscr{L} \ll \lambda = v/f$. This simple but approximate model, illustrated in Fig. 7.11, can be used to obtain a simple approximate model for the time-domain results. Essentially we must require that the significant spectral components of the waveform such as that of a uniform plane wave, $\mathscr{E}_0(t)$, lie below this frequency. In the time domain, this requires that, for example, for a trapezoidal waveform the pulse rise/fall times be much longer than the line's one-way delay, i.e., $\tau_r, \tau_f \gg T$. If this is the case, the frequency-domain forcing functions for a uniform plane-wave excitation given in (7.135) approximate to

$$\hat{V}_F\left(\frac{\mathscr{L}}{2}\right)\mathscr{L} \cong A\left(\frac{1}{v_z}e_x - \frac{1}{v_x}e_z\right)j\omega\hat{E}_0(\omega) \tag{7.194a}$$

$$\hat{I}_F\left(\frac{\mathscr{L}}{2}\right)\mathscr{L} \cong -ce_x A \quad j\omega\hat{E}_0(\omega) \tag{7.194b}$$

where the area of the loop formed by the line is denoted as $A = d\mathscr{L}$. Recognizing that

$$j\omega \Leftrightarrow \frac{\mathrm{d}}{\mathrm{dt}} \tag{7.195}$$

gives the time-domain values of these sources as

$$V_F\left(\frac{\mathscr{L}}{2}, t\right)\mathscr{L} \cong A\left(\frac{1}{v_z}e_x - \frac{1}{v_x}e_z\right)\frac{d\mathscr{E}_0(t)}{dt} \tag{7.196a}$$

$$I_F\left(\frac{\mathscr{L}}{2}, t\right)\mathscr{L} \cong -ce_x A\frac{d\mathscr{E}_0(t)}{dt} \tag{7.196b}$$

For the case of a ground plane, replace the loop area with $A = 2h\mathscr{L}$. The time-domain terminal voltages of the line are obtained from the circuit of Fig. 7.11 as

$$V(0, t) = -\frac{R_S}{R_S + R_L} V_F\left(\frac{\mathscr{L}}{2}, t\right) + \frac{R_S R_L}{R_S + R_L} I_F\left(\frac{\mathscr{L}}{2}, t\right) \tag{7.197a}$$

$$V(\mathscr{L}, t) = \frac{R_L}{R_S + R_L} V_F\left(\frac{\mathscr{L}}{2}, t\right) + \frac{R_S R_L}{R_S + R_L} I_F\left(\frac{\mathscr{L}}{2}, t\right) \tag{7.197b}$$

Again, if the limits on validity of this result are observed (rise/fall times much longer than the line one-way delay), reasonably accurate time-domain predictions can be obtained with minimal computational effort.

7.3.1.5 A SPICE Equivalent Circuit In this section we will describe a simple SPICE model for computing the response of a lossless, two-conductor transmission line to an incident uniform plane wave. This will be extended to the MTL case in subsequent sections.

The frequency-domain chain parameters are given in (7.153):

$$\hat{V}(\mathscr{L}) = \hat{\phi}_{11}(\mathscr{L})\hat{V}(0) + \hat{\phi}_{12}(\mathscr{L})\hat{I}(0) + \hat{V}_{FT}(\mathscr{L}) \tag{7.153a}$$

$$\hat{I}(\mathscr{L}) = \hat{\phi}_{21}(\mathscr{L})\hat{V}(0) + \hat{\phi}_{22}(\mathscr{L})\hat{I}(0) + \hat{I}_{FT}(\mathscr{L}) \tag{7.153b}$$

These illustrate that one model of the line consists of the unexcited line in series with a voltage and a current source representing the effects of the incident field as illustrated in Fig. 7.18(b). Thus one form of a possible SPICE model consists of the usual unexcited line already available in SPICE in cascade with the time-domain sources, $V_{FT}(\mathscr{L}, t) \Leftrightarrow \hat{V}_{FT}(\mathscr{L})$ and $I_{FT}(\mathscr{L}, t) \Leftrightarrow \hat{I}_{FT}(\mathscr{L})$ as illustrated in Fig. 7.18(c). We now examine this possible model. These time-domain sources are derived, for an incident uniform plane wave, as the convolution of the pulse function, $p(t)$, and the functions $V(t)$ and $I(t)$ as shown in (7.180) and (7.181). It was pointed out there that so long as the line cross-sectional dimensions are significantly less than one wavelength at the significant frequencies of the spectrum of the incident waveform, $\mathscr{E}_0(t)$, the pulse function approximates an impulse function, and we obtain, with good approximation,

$$V_{FT}(t) \cong V(t) \tag{7.198a}$$

$$I_{FT}(t) \cong I(t) \tag{7.198b}$$

where $V(t)$ and $I(t)$ are given in (7.178) and (7.179). However, this implementation has a significant problem in that both of these require that we obtain $\mathscr{E}_0(t)$ *advanced in time* as $\mathscr{E}_0(t + T)$! The other functions of $\mathscr{E}_0(t)$ in $V(t)$ and $I(t)$ require only that we delay $\mathscr{E}_0(t)$ as $\mathscr{E}_0(t - T)$ and $\mathscr{E}_0(t - T_z)$ which can be accomplished by simply applying $\mathscr{E}_0(t)$ to an ideal matched line having the appropriate time

delay. The ideal delay line is readily available in SPICE but one to advance a function in time is not. So we next address a more viable model.

Another possible structure for the SPICE model results from the form of the solution given in (7.161):

$$V(0,t) - Z_C I(0,T) = [V(\mathscr{L}, t-T) - Z_C I(\mathscr{L}, t-T)] + V_0(t) \tag{7.199a}$$

$$V(\mathscr{L},t) + Z_C I(\mathscr{L},t) = [V(0, t-T) + Z_C I(0, t-T)] + V_{\mathscr{L}}(t) \tag{7.199b}$$

where

$$\begin{aligned} V_0(t) &= -[V_{FT}(\mathscr{L}, t-T) - Z_C I_{FT}(\mathscr{L}, t-T)] \\ &\cong -[V(t-T) - Z_C I(t-T)] \\ &= -d\left[e_x - e_z\left(\frac{\mathscr{L}}{v_x(T_z+T)}\right)\right][\mathscr{E}_0(t) - \mathscr{E}_0(t-T-T_z)] \end{aligned} \tag{7.200a}$$

$$\begin{aligned} V_{\mathscr{L}}(t) &= [V_{FT}(\mathscr{L}, t) + Z_C I_{FT}(\mathscr{L}, t)] \\ &\cong [V(t) + Z_C I(t)] \\ &= d\left[e_x - e_z\left(\frac{\mathscr{L}}{v_x(T_z-T)}\right)\right][\mathscr{E}_0(t-T) - \mathscr{E}_0(t-T_z)] \end{aligned} \tag{7.200b}$$

Observe that these sources only require that we obtain delayed versions of $\mathscr{E}_0(t)$. This suggests the usual model of an unexcited line containing time-delayed voltage sources. The problem is that we do not have access to internal nodes of the usual SPICE transmission model so that we may add the sources in (7.200) in series with the ones already present (see Fig. 5.8) according to (7.199). The remedy here is simply to build the model using ideal delay lines and controlled sources. Such a model is shown in Fig. 7.20. The external terminals of the line are denoted as 101 and 202 with the 0 node being common. The controlled sources in that model are obtained as

$$E_0(t) = V(2) - d\left[e_x - e_z\left(\frac{\mathscr{L}}{v_x(T_z+T)}\right)\right][V(100) - V(6)] \tag{7.201a}$$

$$E_{\mathscr{L}}(t) = V(4) + d\left[e_x - e_z\left(\frac{\mathscr{L}}{v_x(T_z-T)}\right)\right][V(5) - V(7)] \tag{7.201b}$$

where the usual SPICE designations for the voltage of node n is denoted as $V(n)$. The reader can observe that the circuit of Fig. 7.20 with the controlled source parameters given in (7.201) yields equations (7.199) and (7.200) and is therefore an exact representation. The characteristic impedances Z_{C1}, Z_{C2}, Z_{C3}, Z_{C4}, Z_{C5} in the five auxiliary delay lines need not equal the characteristic impedances of the original line, Z_C, but each line must be appropriately matched

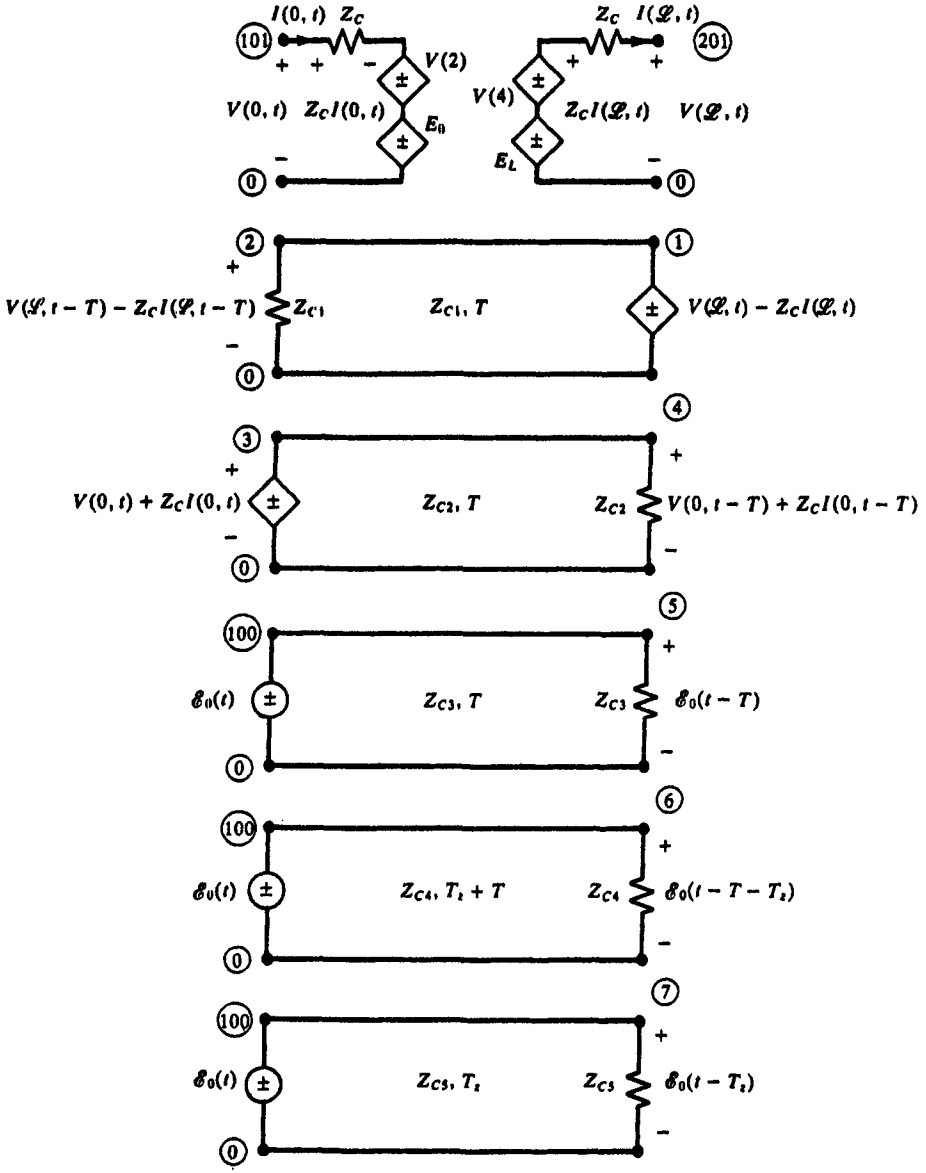

FIGURE 7.20 The SPICE model representing incident-field illumination of a two-conductor line.

to its chosen characteristic impedance to prevent reflections on that line and provide for an ideal delay. The velocities of propagation and line lengths (or equivalently the line time delays) must be as shown. If the incident wave has no z component of its propagation vector, i.e., it is propagating solely in the

x–y plane, then $v_z = \infty$ so that $T_z = 0$ and the last two delay lines in Fig. 7.20 are removed. Similarly, if the wave is propagating solely in the z direction, $T_z = \pm T$, then one term in (7.201) is removed since it also contains $v_x = \infty$. This basic model will be extended to the MTL case in a subsequent section by decoupling the MTL equations.

*7.3.1.6 **Computed Results*** In order to illustrate the accuracy of the SPICE model and to provide an understanding of the relationship between the time-domain parameters of the incident field waveform, $\mathscr{E}_0(t)$, such as rise/fall time we will consider the example shown in Fig. 7.21. A wire of radius $r_w = 10$ mils and length $\mathscr{L} = 1$ m is suspended at a height $h = 2$ cm above an infinite ground plane. The terminations are resistive with $R_S = 500\ \Omega$ and $R_L = 1000\ \Omega$. A uniform plane wave is incident from above ($e_x = 0$, $e_z = 1$, $v_x = -v$, $v_z = \infty$) and has a 1 V/m amplitude and various risetimes. The line characteristic impedance is $Z_C = 303.347\,82\ \Omega$ and the line one-way delay is $T = 3.33564$ ns. We will consider three cases for the risetime: $\tau_r = 50$ ns, $\tau_r = 10$ ns, $\tau_r = 1$ ns. This will illustrate cases where the risetime is greater than or less than the line one-way delay.

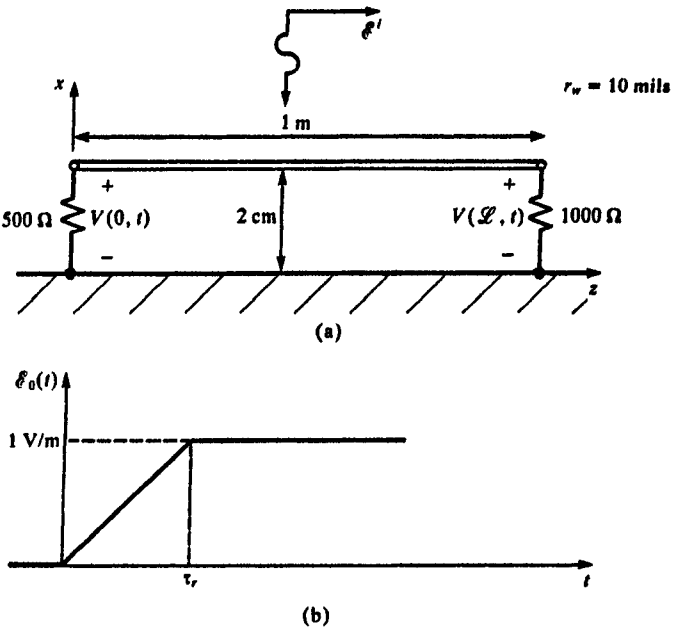

FIGURE 7.21 Characterization of a two-conductor line for illustration of numerical results.

We will compare the predictions of four models:

1. The SPICE model described in the previous section and illustrated in Fig. 7.20.
2. The series solution given by (7.192) using seven terms.
3. The time-domain to frequency-domain transformation method described in Chapter 5.
4. The finite difference–time domain (FDTD) method also described in Chapter 5.

The FDTD method will be discussed in more detail for the case of incident-field illumination in a subsequent section. For the SPICE model, the conductor separation, d, in (7.201) should be replaced by $2h$ since the problem is above a ground plane for reasons discussed previously. This also applies to the series solution parameters given in (7.193). Also because $v_z = \infty$, and $v_x = -v$, the terms containing these in (7.201) are ± 1, and thus lines 4 and 5 containing v_z in Fig. 7.20 are removed from the model. The time-domain to frequency-domain transformation technique simply views the problem as a two port with $\mathscr{E}_0(t)$ as the input and $V(0, t)$ as the output. The incident waveform, $\mathscr{E}_0(t)$, is modeled as a 1 MHz, periodic trapezoidal waveform with equal rise and fall times. The frequency of this waveform is sufficiently long with respect to the transient behavior of the result that the response to the leading edge should be the same as to the actual waveform. The frequency-domain transfer function was computed at 500 harmonics of the basic repetition rate of 1 MHz using the frequency-domain code **INCIDENT.FOR** described in Appendix A. These were combined with the spectral amplitudes and phase angles of the periodic waveform as described in Chapter 5 using the code **TIMEFREQ.FOR** that was used earlier and is also described in Appendix A. In fact, this process is no different from the case where the excitation resides in a termination; the frequency response contains this information. The FDTD solution divides the line into *NDZ* discrete sections and the time variable into *NDT* divisions. The FDTD results were obtained with the **FDTDINC.FOR** code described later. The transmission-line equations in (7.139) are discretized, and the solution is obtained recursively. Again the implementation of the FDTD method is virtually identical to the case of no incident-field excitation described in Chapter 5.

Figure 7.22(a) shows the result for a risetime of $\tau_r = 50$ ns. The SPICE model, the series result, and the time-domain to frequency-domain transformation method using 500 harmonics all give virtually identical results. The time-domain to frequency-domain transformation method using only 100 harmonics is not so accurate. As discussed in Chapter 5, the high-frequency behavior of this waveform rolls off at -40 dB/decade above $1/\pi\tau_r = 6.37$ MHz. Although the final harmonic used, 100 MHz, seems well above this, we evidently require more harmonics to give adequate time-domain predictions with this method. The

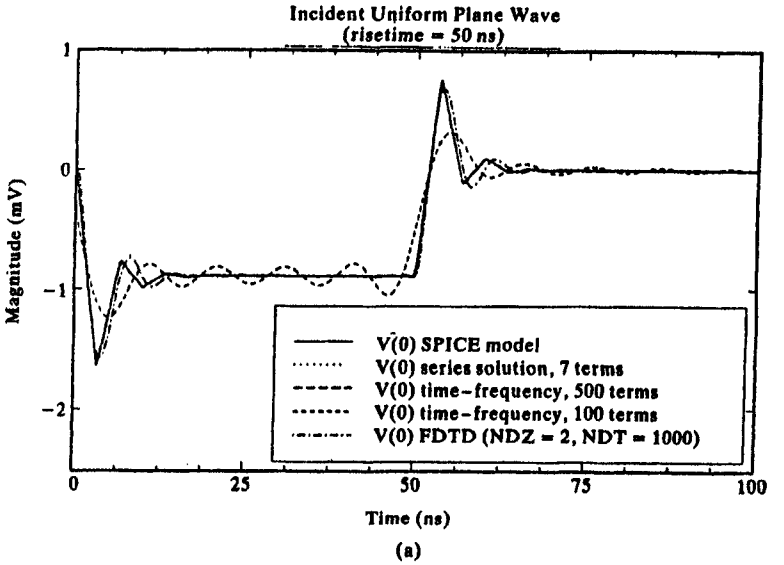

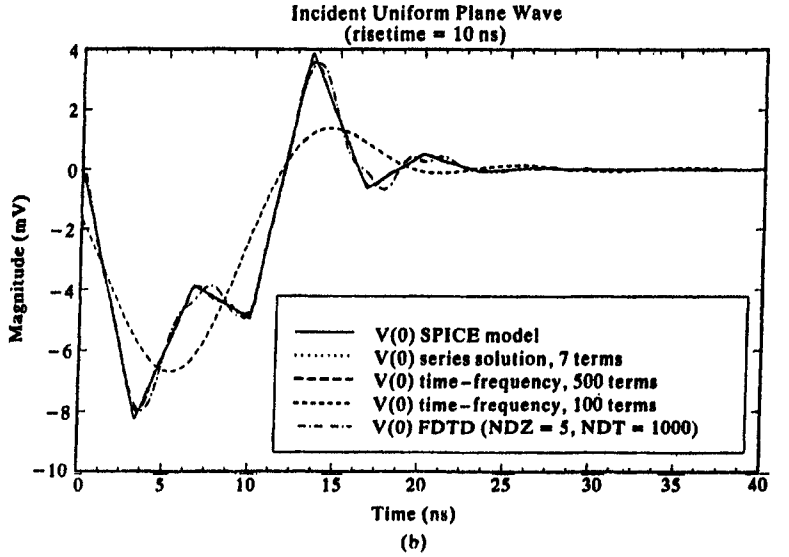

FIGURE 7.22 Predictions of the time-domain near-end voltage of the line of Fig. 7.21 using the SPICE model, the series solution, the time-domain to frequency-domain transformation method, and the FDTD method for an incident uniform plane wave with a risetime of (a) 50 ns, (b) 10 ns, and (c) 1 ns.

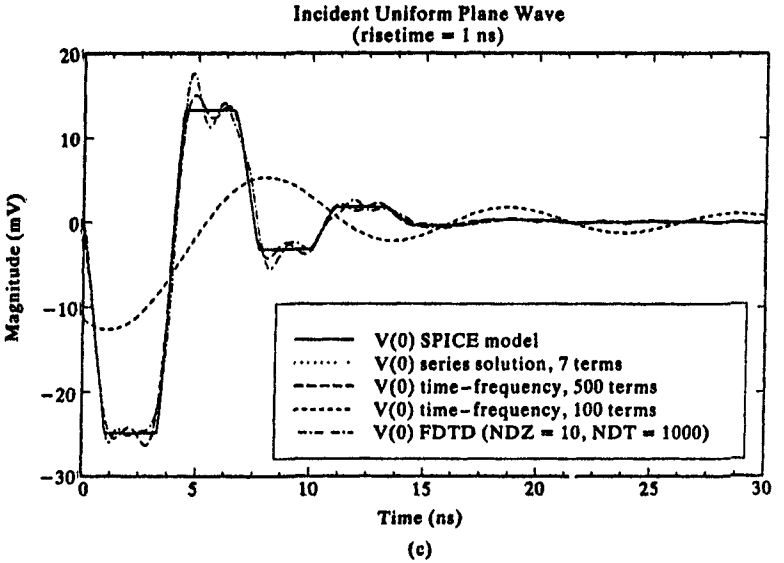

FIGURE 7.22 (*continued*)

FDTD results using $NDZ = 2$ and $NDT = 1000$ also give accurate predictions. This is to be expected since dividing the line into two sections means each section is one-tenth of a wavelength at 30 MHz. Observe that the resulting waveform appears to be related to the *derivative* of $\mathscr{E}_0(t)$. In fact, this is the case for this sufficiently long risetime. One can compute from the results for an electrically short line given in (7.197) an expected level of $V(0, t) \cong -0.889$ mV which is exactly the level computed by the other exact methods. Here the risetime is more than $10T$ so the result is expected. Figure 7.22(b) shows the result for a risetime of $\tau_r = 10$ ns. Again all four methods (using 500 harmonics) give virtually identical results. However, the risetime is of the order of the line one-way delay so that the result no longer resembles the derivative of $\mathscr{E}_0(t)$ as expected. Figure 7.22(c) shows the result for a risetime of $\tau_r = 1$ ns. The SPICE model and the series solution again give virtually identical results. The time-domain to frequency-domain transformation method even using 500 harmonics is beginning to show errors. Here the high-frequency spectrum of $\mathscr{E}_0(t)$ rolls off at -40 dB/decade above 318 MHz so we would expect the results using only 500 harmonics to be inadequate. Similarly, the FDTD solution shows some ringing in its solution.

7.3.2 Multiconductor Lines

We now apply many of the notions developed for two-conductor lines to the case of lossless MTL's. The primary method will again be to uncouple the MTL equations via similarity transformations. This yields n uncoupled two-conductor

lines which can be modeled using all of the previous techniques. In particular, a simple SPICE model will be developed. In addition, there are several other direct methods that will be discussed: lumped-circuit iterative models, time-domain to frequency-domain transformations, and finite difference–time domain (FDTD) methods.

7.3.2.1 Decoupling the MTL Equations Diagonalization of the MTL equations as in Chapter 5 is a viable method for lossless lines. Consider the MTL equations for a lossless line:

$$\frac{\partial}{\partial z}\mathbf{V}(z,t) = -\mathbf{L}\frac{\partial}{\partial t}\mathbf{I}(z,t) + \mathbf{V}_F(z,t) \tag{7.202a}$$

$$\frac{\partial}{\partial z}\mathbf{I}(z,t) = -\mathbf{C}\frac{\partial}{\partial t}\mathbf{V}(z,t) + \mathbf{I}_F(z,t) \tag{7.202b}$$

In a fashion virtually identical to the technique of Chapter 5, define the transformation to *mode* quantities as

$$\mathbf{V}(z,t) = \mathbf{T}_V\mathbf{V}_m(z,t) \tag{7.203a}$$

$$\mathbf{I}(z,t) = \mathbf{T}_I\mathbf{I}_m(z,t) \tag{7.203b}$$

Substituting these into (7.202) gives

$$\frac{\partial}{\partial z}\mathbf{V}_m(z,t) = -\mathbf{L}_m\frac{\partial}{\partial t}\mathbf{I}_m(z,t) + \mathbf{V}_{Fm}(z,t) \tag{7.204a}$$

$$\frac{\partial}{\partial z}\mathbf{I}_m(z,t) = -\mathbf{C}_m\frac{\partial}{\partial t}\mathbf{V}_m(z,t) + \mathbf{I}_{Fm}(z,t) \tag{7.204b}$$

where $\mathbf{L}_m$ and $\mathbf{C}_m$ are the $n \times n$ matrices

$$\mathbf{L}_m = \mathbf{T}_V^{-1}\mathbf{L}\mathbf{T}_I \tag{7.205a}$$

$$\mathbf{C}_m = \mathbf{T}_I^{-1}\mathbf{C}\mathbf{T}_V \tag{7.205b}$$

and the incident-field forcing functions for the *modes* become

$$\mathbf{V}_{Fm}(z,t) = \mathbf{T}_V^{-1}\mathbf{V}_F(z,t) \tag{7.206a}$$

$$\mathbf{I}_{Fm}(z,t) = \mathbf{T}_I^{-1}\mathbf{I}_F(z,t) \tag{7.206b}$$

If $\mathbf{T}_V$ and $\mathbf{T}_I$ can be chosen such that $\mathbf{L}_m$ and $\mathbf{C}_m$ are *diagonal* matrices, then the equations become uncoupled sets of two-conductor lines each with incident-field excitation through elements of the vectors $\mathbf{V}_{FM}(z,t)$ and $\mathbf{I}_{Fm}(z,t)$. This can

always be done for lossless lines as was shown in Chapters 4 and 5. So the basic solution technique utilizes the solution for a field-illuminated, lossless two-conductor line which was obtained previously. As discussed in Section 5.2.1.2, a suitable transformation can be found which accomplishes this. This transformation is obtained by first determining a real orthogonal transformation $\mathbf{U}$ that diagonalizes $\mathbf{C}$ as

$$\mathbf{U}^t\mathbf{C}\mathbf{U} = \boldsymbol{\theta}^2 \tag{7.207}$$

where $\boldsymbol{\theta}^2$ is a diagonal matrix and $\mathbf{U}^t$ denotes the *transpose of* $\mathbf{U}$. Since $\mathbf{C}$ is real and symmetric, this can always be done. Furthermore, since $\mathbf{C}$ is positive definite, all elements of $\boldsymbol{\theta}^2$ are real and positive so that we can form the square root of that matrix, $\boldsymbol{\theta}$, which will have real elements on its main diagonal and zeros elsewhere. Next find a real orthogonal transformation, $\mathbf{S}$, such that

$$\mathbf{S}^t(\boldsymbol{\theta}\mathbf{U}^t\mathbf{L}\mathbf{U}\boldsymbol{\theta})\mathbf{S} = \boldsymbol{\Lambda}^2 \tag{7.208}$$

where $\boldsymbol{\Lambda}^2$ is again a *diagonal* matrix with real positive elements on its diagonal. Define

$$\mathbf{T} = \mathbf{U}\boldsymbol{\theta}\mathbf{S} \tag{7.209}$$

Normalizing the columns of $\mathbf{T}$ to unit length gives

$$\mathbf{T}_{\text{norm}} = \mathbf{T}\boldsymbol{\alpha} \tag{7.210}$$

where $\boldsymbol{\alpha}$ is an $n \times n$ diagonal matrix. The above transformations can now be defined as

$$\mathbf{T}_I = \mathbf{U}\boldsymbol{\theta}\mathbf{S}\boldsymbol{\alpha} \tag{7.211}$$

$$\mathbf{T}_V = \mathbf{U}\boldsymbol{\theta}^{-1}\mathbf{S}\boldsymbol{\alpha}^{-1} \tag{7.212}$$

with the property that

$$\begin{aligned}\mathbf{T}_V^{-1} &= \boldsymbol{\alpha}^2\mathbf{T}_I^{-1}\mathbf{C} \\ &= \mathbf{T}_I^t\end{aligned} \tag{7.213}$$

The modal per-unit-length parameter matrices given in (7.205) become

$$\begin{aligned}\mathbf{L}_m &= \mathbf{T}_V^{-1}\mathbf{L}\mathbf{T}_I \\ &= \mathbf{T}_I^t\mathbf{L}\mathbf{T}_I \\ &= \boldsymbol{\alpha}^2\boldsymbol{\Lambda}^2\end{aligned} \tag{7.214a}$$

$$\begin{aligned}\mathbf{C}_m &= \mathbf{T}_I^{-1}\mathbf{C}\mathbf{T}_V \\ &= \mathbf{T}_V^t\mathbf{C}\mathbf{T}_V \\ &= \boldsymbol{\alpha}^{-2}\end{aligned} \tag{7.214b}$$

Consequently the mode characteristic impedances and velocities of propagation become

$$[Z_{Cm}]_l = Z_{Cml} \tag{7.215a}$$
$$= \sqrt{\frac{l_{ml}}{c_{ml}}}$$
$$= \alpha_l^2 \Lambda_l$$
$$v_{ml} = \frac{1}{\sqrt{l_{ml} c_{ml}}} \tag{7.215b}$$
$$= \frac{1}{\Lambda_l}$$

In order to obtain the time-domain solutions, we again transform the frequency-domain chain parameter matrix to the time domain. The frequency-domain chain parameter matrix relates the phasor voltages and currents at one end of the line to those at the other as

$$\hat{\mathbf{V}}(\mathscr{L}) = \hat{\mathbf{\Phi}}_{11}(\mathscr{L})\hat{\mathbf{V}}(0) + \hat{\mathbf{\Phi}}_{12}(\mathscr{L})\hat{\mathbf{I}}(0) + \hat{\mathbf{V}}_{FT}(\mathscr{L}) \tag{7.216a}$$
$$\hat{\mathbf{I}}(\mathscr{L}) = \hat{\mathbf{\Phi}}_{21}(\mathscr{L})\hat{\mathbf{V}}(0) + \hat{\mathbf{\Phi}}_{22}(\mathscr{L})\hat{\mathbf{I}}(0) + \hat{\mathbf{I}}_{FT}(\mathscr{L}) \tag{7.216b}$$

where the total forcing functions are given by

$$\hat{\mathbf{V}}_{FT}(\mathscr{L}) = \int_0^{\mathscr{L}} [\hat{\mathbf{\Phi}}_{11}(\mathscr{L} - \tau)\hat{\mathbf{V}}_F(\tau) + \hat{\mathbf{\Phi}}_{12}(\mathscr{L} - \tau)\hat{\mathbf{I}}_F(\tau)]\, d\tau \tag{7.217a}$$

$$\hat{\mathbf{I}}_{FT}(\mathscr{L}) = \int_0^{\mathscr{L}} [\hat{\mathbf{\Phi}}_{21}(\mathscr{L} - \tau)\hat{\mathbf{V}}_F(\tau) + \hat{\mathbf{\Phi}}_{22}(\mathscr{L} - \tau)\hat{\mathbf{I}}_F(\tau)]\, d\tau \tag{7.217b}$$

and the chain parameter submatrices are

$$\hat{\mathbf{\Phi}}_{11}(\mathscr{L}) = \tfrac{1}{2}\mathbf{C}^{-1}\mathbf{T}_I(\mathbf{e}^{j\omega\Lambda\mathscr{L}} + \mathbf{e}^{-j\omega\Lambda\mathscr{L}})\mathbf{T}_I^{-1}\mathbf{C} \tag{7.218a}$$
$$\hat{\mathbf{\Phi}}_{12}(\mathscr{L}) = -\tfrac{1}{2}\mathbf{C}^{-1}\mathbf{T}_I\Lambda(\mathbf{e}^{j\omega\Lambda\mathscr{L}} - \mathbf{e}^{-j\omega\Lambda\mathscr{L}})\mathbf{T}_I^{-1} \tag{7.218b}$$
$$\hat{\mathbf{\Phi}}_{21}(\mathscr{L}) = -\tfrac{1}{2}\mathbf{T}_I(\mathbf{e}^{j\omega\Lambda\mathscr{L}} - \mathbf{e}^{-j\omega\Lambda\mathscr{L}})\Lambda^{-1}\mathbf{T}_I^{-1}\mathbf{C} \tag{7.218c}$$
$$\hat{\mathbf{\Phi}}_{22}(\mathscr{L}) = \tfrac{1}{2}\mathbf{T}_I(\mathbf{e}^{j\omega\Lambda\mathscr{L}} + \mathbf{e}^{-j\omega\Lambda\mathscr{L}})\mathbf{T}_I^{-1} \tag{7.218d}$$

where $\mathbf{e}^{\pm j\omega\Lambda\mathscr{L}}$ are diagonal matrices with $e^{\pm j\omega\Lambda_l\mathscr{L}}$ on the main diagonals and $\mathbf{T}_I^{-1}\mathbf{C}\mathbf{L}\mathbf{T}_I = \Lambda^2$. Transforming to mode quantities yields

$$\hat{\mathbf{V}}_m(\mathscr{L}) = \hat{\mathbf{\Phi}}_{m11}(\mathscr{L})\hat{\mathbf{V}}_m(0) + \hat{\mathbf{\Phi}}_{m12}(\mathscr{L})\hat{\mathbf{I}}_m(0) + \hat{\mathbf{V}}_{FTm}(\mathscr{L}) \tag{7.219a}$$
$$\hat{\mathbf{I}}_m(\mathscr{L}) = \hat{\mathbf{\Phi}}_{m21}(\mathscr{L})\hat{\mathbf{V}}_m(0) + \hat{\mathbf{\Phi}}_{m22}(\mathscr{L})\hat{\mathbf{I}}_m(0) + \hat{\mathbf{I}}_{FTm}(\mathscr{L}) \tag{7.219b}$$

where the modal chain parameter submatrices are

$$\hat{\Phi}_{m11}(\mathscr{L}) = \mathbf{T}_V^{-1}\hat{\Phi}_{11}(\mathscr{L})\mathbf{T}_V = \tfrac{1}{2}(e^{j\omega\Lambda\mathscr{L}} + e^{-j\omega\Lambda\mathscr{L}}) \tag{7.220a}$$

$$\hat{\Phi}_{m12}(\mathscr{L}) = \mathbf{T}_V^{-1}\hat{\Phi}_{12}(\mathscr{L})\mathbf{T}_I = \underbrace{-\tfrac{1}{2}\alpha^2\Lambda}_{\mathbf{Z}_{Cm}}(e^{j\omega\Lambda\mathscr{L}} - e^{-j\omega\Lambda\mathscr{L}}) \tag{7.220b}$$

$$\hat{\Phi}_{m21}(\mathscr{L}) = \mathbf{T}_I^{-1}\hat{\Phi}_{21}(\mathscr{L})\mathbf{T}_V = -\tfrac{1}{2}(e^{j\omega\Lambda\mathscr{L}} - e^{-j\omega\Lambda\mathscr{L}})\underbrace{\alpha^{-2}\Lambda^{-1}}_{\mathbf{Z}_{Cm}^{-1}} \tag{7.220c}$$

$$\hat{\Phi}_{m22}(\mathscr{L}) = \mathbf{T}_I^{-1}\hat{\Phi}_{22}(\mathscr{L})\mathbf{T}_I = \tfrac{1}{2}(e^{j\omega\Lambda\mathscr{L}} + e^{-j\omega\Lambda\mathscr{L}}) \tag{7.220d}$$

and the total modal forcing functions due to the incident field become

$$\begin{aligned}\hat{\mathbf{V}}_{FTm}(\mathscr{L}) &= \mathbf{T}_V^{-1}\hat{\mathbf{V}}_{FT}(\mathscr{L}) \\ &= \int_0^{\mathscr{L}} [\hat{\Phi}_{m11}(\mathscr{L}-\tau)\hat{\mathbf{V}}_F(\tau) + \hat{\Phi}_{m12}(\mathscr{L}-\tau)\hat{\mathbf{I}}_F(\tau)]\,d\tau \\ &= \int_0^{\mathscr{L}} [\tfrac{1}{2}(e^{j\omega\Lambda(\mathscr{L}-\tau)} + e^{-j\omega\Lambda(\mathscr{L}-\tau)})\hat{\mathbf{V}}_F(\tau) \\ &\qquad - \tfrac{1}{2}(e^{j\omega\Lambda(\mathscr{L}-\tau)} - e^{-j\omega\Lambda(\mathscr{L}-\tau)})\mathbf{Z}_{Cm}\hat{\mathbf{I}}_F(\tau)]\,d\tau\end{aligned} \tag{7.221a}$$

$$\begin{aligned}\hat{\mathbf{I}}_{FTm}(\mathscr{L}) &= \mathbf{T}_I^{-1}\hat{\mathbf{I}}_{FT}(\mathscr{L}) \\ &= \int_0^{\mathscr{L}} [\hat{\Phi}_{m21}(\mathscr{L}-\tau)\hat{\mathbf{V}}_F(\tau) + \hat{\Phi}_{m22}(\mathscr{L}-\tau)\hat{\mathbf{I}}_F(\tau)]\,d\tau \\ &= \int_0^{\mathscr{L}} [-\tfrac{1}{2}(e^{j\omega\Lambda(\mathscr{L}-\tau)} - e^{-j\omega\Lambda(\mathscr{L}-\tau)})\mathbf{Z}_{Cm}^{-1}\hat{\mathbf{V}}_F(\tau) \\ &\qquad + \tfrac{1}{2}(e^{j\omega\Lambda(\mathscr{L}-\tau)} + e^{-j\omega\Lambda(\mathscr{L}-\tau)})\hat{\mathbf{I}}_F(\tau)]\,d\tau\end{aligned} \tag{7.221b}$$

7.3.2.2 A SPICE Equivalent Circuit We now obtain the time-domain version of the chain parameter representation. This will show how to construct a time-domain equivalent circuit that is implementable in the SPICE program. Substituting (7.220) into (7.219) yields

$$\hat{\mathbf{V}}_m(\mathscr{L}) = \tfrac{1}{2}(e^{j\omega\Lambda\mathscr{L}} + e^{-j\omega\Lambda\mathscr{L}})\hat{\mathbf{V}}_m(0) - \tfrac{1}{2}(e^{j\omega\Lambda\mathscr{L}} - e^{-j\omega\Lambda\mathscr{L}})\mathbf{Z}_{Cm}\hat{\mathbf{I}}_m(0) + \hat{\mathbf{V}}_{FTm}(\mathscr{L}) \tag{7.222a}$$

$$\mathbf{Z}_{Cm}\hat{\mathbf{I}}_m(\mathscr{L}) = -\tfrac{1}{2}(e^{j\omega\Lambda\mathscr{L}} - e^{-j\omega\Lambda\mathscr{L}})\hat{\mathbf{V}}_m(0) + \tfrac{1}{2}(e^{j\omega\Lambda\mathscr{L}} + e^{-j\omega\Lambda\mathscr{L}})\mathbf{Z}_{Cm}\hat{\mathbf{I}}_m(0) + \mathbf{Z}_{Cm}\hat{\mathbf{I}}_{FTm}(\mathscr{L}) \tag{7.222b}$$

Adding and subtracting these yields

$$\hat{\mathbf{V}}_m(0) - \mathbf{Z}_{Cm}\hat{\mathbf{I}}_m(0) = e^{-j\omega\Lambda\mathscr{L}}[\hat{\mathbf{V}}_m(\mathscr{L}) - \mathbf{Z}_{Cm}\hat{\mathbf{I}}_m(\mathscr{L})] + \hat{\mathbf{E}}_0(\mathscr{L}) \tag{7.223a}$$

$$\hat{\mathbf{V}}_m(\mathscr{L}) + \mathbf{Z}_{Cm}\hat{\mathbf{I}}_m(\mathscr{L}) = e^{-j\omega\Lambda\mathscr{L}}[\hat{\mathbf{V}}_m(0) + \mathbf{Z}_{Cm}\hat{\mathbf{I}}_m(0)] + \hat{\mathbf{E}}_{\mathscr{L}}(\mathscr{L}) \tag{7.223b}$$

where

$$\hat{\mathbf{E}}_0(\mathscr{L}) = -e^{-j\omega\Lambda\mathscr{L}}[\hat{\mathbf{V}}_{FTm}(\mathscr{L}) - \mathbf{Z}_{Cm}\hat{\mathbf{I}}_{FTm}(\mathscr{L})] \tag{7.224a}$$

$$\hat{\mathbf{E}}_{\mathscr{L}}(\mathscr{L}) = [\hat{\mathbf{V}}_{FTm}(\mathscr{L}) + \mathbf{Z}_{Cm}\hat{\mathbf{I}}_{FTm}(\mathscr{L})] \tag{7.224b}$$

Recognizing the basic time-delay transformation:

$$e^{\pm j\omega T}\hat{F}(\omega) \Leftrightarrow F(t - T) \tag{7.225}$$

these become, in the time domain,

$$[\mathbf{V}_m(0, t) - \mathbf{Z}_{Cm}\mathbf{I}_m(0, t)]_l = [\mathbf{V}_m(\mathscr{L}, t - T_l) - \mathbf{Z}_{Cm}\mathbf{I}_m(\mathscr{L}, t - T_l)]_l + [\mathbf{E}_0(t)]_l \tag{7.226a}$$

$$[\mathbf{V}_m(\mathscr{L}, t) + \mathbf{Z}_{Cm}\mathbf{I}_m(\mathscr{L}, t)]_l = [\mathbf{V}_m(0, t - T_l) + \mathbf{Z}_{Cm}\mathbf{I}_m(0, t - T_l)]_l + [\mathbf{E}_{\mathscr{L}}(t)]_l \tag{7.226b}$$

where we denote the i-th entry in a vector $\mathbf{V}$ as $[\mathbf{V}]_i$, and the one-way time delay of the i-th modal line is denoted by

$$T_l = \frac{\mathscr{L}}{v_{ml}} = \Lambda_l\mathscr{L} \tag{7.227}$$

The additional sources are

$$[\mathbf{E}_0(t)]_l = -[\mathbf{V}_{FTm}(\mathscr{L}, t - T_l) - \mathbf{Z}_{Cm}\mathbf{I}_{FTm}(\mathscr{L}, t - T_l)]_l \tag{7.228a}$$

$$[\mathbf{E}_{\mathscr{L}}(t)]_l = [\mathbf{V}_{FTm}(\mathscr{L}, t) + \mathbf{Z}_{Cm}\mathbf{I}_{FTm}(\mathscr{L}, t)]_l \tag{7.228b}$$

Equations (7.226) suggest the usual SPICE equivalent circuit for the modes where we add to it the sources due to the incident field, $[\mathbf{E}_0(t)]_l$ and $[\mathbf{E}_{\mathscr{L}}(t)]_l$. The transformation back to the actual line voltages and currents is accomplished

with controlled sources that represent the mode transformations according to (7.203):

$$[\mathbf{V}(z,t)]_t = \sum_{k=1}^{n} \{[\mathbf{T}_V]_{ik}[\mathbf{V}_m(z,t)]_k\} \tag{7.229a}$$

$$[\mathbf{I}_m(z,t)]_t = \sum_{k=1}^{n} \{[\mathbf{T}_I^{-1}]_{ik}[\mathbf{I}(z,t)]_k\} \tag{7.229b}$$

as in Chapter 5. Thus the only difference between the SPICE model derived for the case of the excitation in the terminal networks and this case, wherein the excitation is via an incident field, is the implementation of the sources due to that field given in (7.221) and (7.226).

Although the above is valid for any time-domain form of the incident field, we will now restrict our attention to uniform plane-wave excitation of the line. The modal forcing functions in (7.224) become

$$\hat{\mathbf{E}}_0(\mathscr{L}) = -\mathbf{e}^{-j\omega\Lambda\mathscr{L}}[\hat{\mathbf{V}}_{FTm}(\mathscr{L}) - \mathbf{Z}_{Cm}\hat{\mathbf{I}}_{FTm}(\mathscr{L})] \tag{7.230a}$$

$$= -\int_0^{\mathscr{L}} \mathbf{e}^{-j\omega\Lambda\tau}\mathbf{T}_I^t\hat{\mathbf{E}}_L(\tau)\,d\tau + \mathbf{e}^{-j\omega\Lambda\tau}\mathbf{T}_I^t\hat{\mathbf{E}}_T(\mathscr{L}) - \mathbf{T}_I^t\hat{\mathbf{E}}_T(0)$$

$$\hat{\mathbf{E}}_{\mathscr{L}}(\mathscr{L}) = [\hat{\mathbf{V}}_{FTm}(\mathscr{L}) + \mathbf{Z}_{Cm}\hat{\mathbf{I}}_{FTm}(\mathscr{L})] \tag{7.230b}$$

$$= \int_0^{\mathscr{L}} \mathbf{e}^{-j\omega\Lambda(\mathscr{L}-\tau)}\mathbf{T}_I^t\hat{\mathbf{E}}_L(\tau)\,d\tau - \mathbf{T}_I^t\hat{\mathbf{E}}_T(\mathscr{L}) + \mathbf{e}^{-j\omega\Lambda\mathscr{L}}\mathbf{T}_I^t\hat{\mathbf{E}}_T(0)$$

where $\hat{\mathbf{E}}_T$ denotes the vector of contributions from the *transverse* electric field, and $\hat{\mathbf{E}}_L$ denotes the vector of contributions from the *longitudinal* electric field. If the reference conductor is placed at the origin of the coordinate system, $x = 0$, $y = 0$, as shown in Fig. 7.7(a), the transverse field contributions can again be written in terms of the cross-sectional coordinates of the k-th conductor (x_k, y_k) using the general form of the incident field in (7.58) as

$$[\hat{\mathbf{E}}_T(\mathscr{L})]_k = \int_a^{a'} \hat{\vec{E}}_{tk}^{\,t}\cdot d\vec{l} \tag{7.231a}$$

$$= \hat{E}_o(e_x x_k + e_y y_k)\frac{\sin(\psi_k)}{\psi_k}\,e^{-j\psi_k}e^{-j\beta_z\mathscr{L}}$$

where $d_k = \sqrt{x_k^2 + y_k^2}$ is the straight-line distance between the reference conductor and the k-th conductor in the transverse plane and

$$\psi_k = \frac{(\beta_x x_k + \beta_y y_k)}{2} \tag{7.231b}$$

Similarly, the contributions due to the longitudinal field are

$$[\hat{\mathbf{E}}_L(z)]_k = \hat{E}_z^i(x_k, y_k, z) - \hat{E}_z^i(0, 0, z) \tag{7.232}$$

$$= -j(\beta_x x_k + \beta_y y_k)\hat{E}_o e_z \frac{\sin(\psi_k)}{\psi_k} e^{-j\psi_k} e^{-j\beta_z z}$$

Denoting the cross-sectional time delay as

$$T_{xyk} = \frac{x_k}{v_x} + \frac{y_k}{v_y} \tag{7.233}$$

and

$$T_z = \frac{\mathscr{L}}{v_z} \tag{7.234}$$

along with the time delay of the modes:

$$T_l = \frac{\mathscr{L}}{v_l} = \Lambda_l \mathscr{L} \tag{7.235}$$

(7.230) becomes

$$[\hat{\mathbf{E}}_0(\mathscr{L})]_i = \hat{E}_o(\omega) \sum_{k=1}^{n} \left\{ \left[\frac{\sin(\psi_k)}{\psi_k} \right] [\mathbf{T}_l^i]_{ik} \right. \tag{7.236a}$$

$$\times [e_z T_{xyk} \mathscr{L} + (e_x x_k + e_y y_k)(T_l - T_z)]$$

$$\left. \times \frac{(e^{-j\omega(T_{xyk}/2)} - e^{-j\omega(T_l + T_z + (T_{xyk}/2))})}{(T_l + T_z)} \right\}$$

$$[\hat{\mathbf{E}}_{\mathscr{L}}(\mathscr{L})]_i = \hat{E}_o(\omega) \sum_{k=1}^{n} \left\{ \left[\frac{\sin(\psi_k)}{\psi_k} \right] [\mathbf{T}_l^i]_{ik} \right. \tag{7.236b}$$

$$\times [e_z T_{xyk} \mathscr{L} + (e_x x_k + e_y y_k)(T_l - T_z)]$$

$$\left. \times \frac{(e^{-j\omega(T_l + (T_{xyk}/2))} - e^{-j\omega(T_z + (T_{xyk}/2))})}{(T_l - T_z)} \right\}$$

Again, recognizing the basic time-delay transformation in (7.225), these sources transform to the time domain as

$$[\mathbf{E}_0(t)]_i = \sum_{k=1}^{n} \left\{ [e_z T_{xyk} \mathscr{L} - (e_x x_k + e_y y_k)(T_l + T_z)][\mathbf{T}_l^i]_{ik} \right. \tag{7.237a}$$

$$\left. \times p_k(t) * \frac{\mathscr{E}_o\left(t - \frac{T_{xyk}}{2}\right) - \mathscr{E}_o\left(t - T_l - T_z - \frac{T_{xyk}}{2}\right)}{(T_l + T_z)} \right\}$$

$$[\mathbf{E}_{\mathscr{L}}(t)]_l = \sum_{k=1}^{n} \left\{ [e_z T_{xyk} \mathscr{L} + (e_x x_k + e_y y_k)(T_l - T_z)][\mathbf{T}_I^t]_{lk} \times p_k(t) * \frac{\mathscr{E}_o\left(t - T_l - \frac{T_{xyk}}{2}\right) - \mathscr{E}_o\left(t - T_z - \frac{T_{xyk}}{2}\right)}{(T_l - T_z)} \right\} \tag{7.237b}$$

where $p_k(t)$ is the pulse function for the k-th conductor given by

$$p_k(t) = \begin{cases} 0 & t < -\dfrac{Txyk}{2} \\ \dfrac{1}{T_{xyk}} & -\dfrac{Txyk}{2} < t < \dfrac{Txyk}{2} \\ 0 & t > -\dfrac{Txyk}{2} \end{cases} \tag{7.238}$$

as illustrated in Fig. 7.19 and $*$ denotes the *convolution* operation. Again, let us assume that the line cross-sectional dimensions are electrically small at the significant frequencies of the waveform, $\mathscr{E}_o(t)$, so that $p_k(t)$ approximates an impulse:

$$p_k(t) \cong \delta(t) \tag{7.239}$$

Similarly we will neglect the cross-sectional time delay in the expressions involving $\mathscr{E}_o(t)$, $T_{xyk} \cong 0$ for all k, so that the forcing functions simplify to

$$\mathbf{E}_0(t) = \alpha_0 \left[\frac{\mathscr{E}_o(t) - \mathscr{E}_o(t - T_l - T_z)}{(T_l + T_z)} \right] \tag{7.240a}$$

$$\mathbf{E}_{\mathscr{L}}(t) = \alpha_{\mathscr{L}} \left[\frac{\mathscr{E}_o(t - T_l) - \mathscr{E}_o(t - T_z)}{(T_l - T_z)} \right] \tag{7.240b}$$

where the entries in the $n \times 1$ vectors α_0 and $\alpha_{\mathscr{L}}$ are given by

$$[\alpha_0]_l = \sum_{k=1}^{n} \{[e_z T_{xyk} \mathscr{L} - (e_x x_k + e_y y_k)(T_l + T_z)][\mathbf{T}_I^t]_{lk}\} \tag{7.241a}$$

$$[\alpha_{\mathscr{L}}]_l = \sum_{k=1}^{n} \{[e_z T_{xyk} \mathscr{L} + (e_x x_k + e_y y_k)(T_l - T_z)][\mathbf{T}_I^t]_{lk}\} \tag{7.241b}$$

Therefore, the modal expressions in (7.226) simplify to

$$[\mathbf{V}_m(0,t) - \mathbf{Z}_{Cm}\mathbf{I}_m(0,t)]_i = [\mathbf{V}_m(\mathscr{L}, t - T_i) - \mathbf{Z}_{Cm}\mathbf{I}_m(\mathscr{L}, t - T_i)]_i + [\alpha_0]_i\left[\frac{\mathscr{E}_o(t) - \mathscr{E}_o(t - T_i - T_z)}{(T_i + T_z)}\right] \quad (7.242a)$$

$$[\mathbf{V}_m(\mathscr{L}, t) + \mathbf{Z}_{Cm}\mathbf{I}_m(\mathscr{L}, t)]_i = [\mathbf{V}_m(0, t - T_i) + \mathbf{Z}_{Cm}\mathbf{I}_m(0, t - T_i)]_i + [\alpha_{\mathscr{L}}]_i\left[\frac{\mathscr{E}_o(t - T_i) - \mathscr{E}_o(t - T_z)}{(T_i - T_z)}\right] \quad (7.242b)$$

Equations (7.242) suggest the SPICE model shown in Fig. 7.23. The external nodes are denoted as 10i (at $z = 0$) and 20i (at $z = \mathscr{L}$). Nodes 30i, 40i, 50i, and 60i attach to controlled sources which implement the transformations between actual and mode quantities given in (7.229). The remainder of the network implements (7.242) for the i-th mode. The five delay lines simulating equation (7.242) for each mode need not be terminated in the mode characteristic impedances but can be terminated in any characteristic impedance in order to remove reflections and give the desired ideal delay of $\mathscr{E}_o(t)$. If the wave has no propagation component in the z direction, $T_z = 0$, then the last two lines are removed from the model. If the wave has a component in the $+z$ direction, it may happen that $T_i = T_z$ in which case (7.242b) appears to be undefined. However, this term becomes

$$\left[\frac{\mathscr{E}_o(t - T_i) - \mathscr{E}_o(t - T_z)}{(T_i - T_z)}\right]_{T_z \to T_i} = \frac{d}{dt}\mathscr{E}_o(t - T_i) \quad (7.243)$$

so that the last delay line is replaced as shown in Fig. 7.24. Waves having a component in the $-z$ direction, may result in the last two delay lines having negative delays which SPICE does not allow. Thus we must restrict this model to positive T_z. For negative T_z simply reverse the ends of the model. This model is implemented via a SPICE subcircuit generated by the FORTRAN program **SPICEINC.FOR** described in Appendix A.

7.3.2.3 Lumped-Circuit Iterative Approximate Characterizations The use of lumped-circuit approximations such as the lumped ⅂, ⌐, π, and T circuits parallels all of the previous such uses. The lumped π and T circuits shown for the phasor, frequency-domain solution in Fig. 7.5 can be used directly for the time-domain solution by simply replacing the phasor sources, $\hat{V}_{Fi}\mathscr{L}$ and $\hat{I}_{Fi}\mathscr{L}$ with their time-domain equivalents, $V_{Fi}\mathscr{L}$ and $I_{Fi}\mathscr{L}$.

7.3.2.4 Time-Domain to Frequency-Domain Transformations Perhaps the most straightforward method of obtaining the time-domain response is to view the problem as a two port with $\mathscr{E}_o(t)$ as the input and the desired terminal response voltage (or current) as the output. The magnitude and phase of $\mathscr{E}_o(t)$ can be obtained with the Fourier transform or can be approximated as a periodic

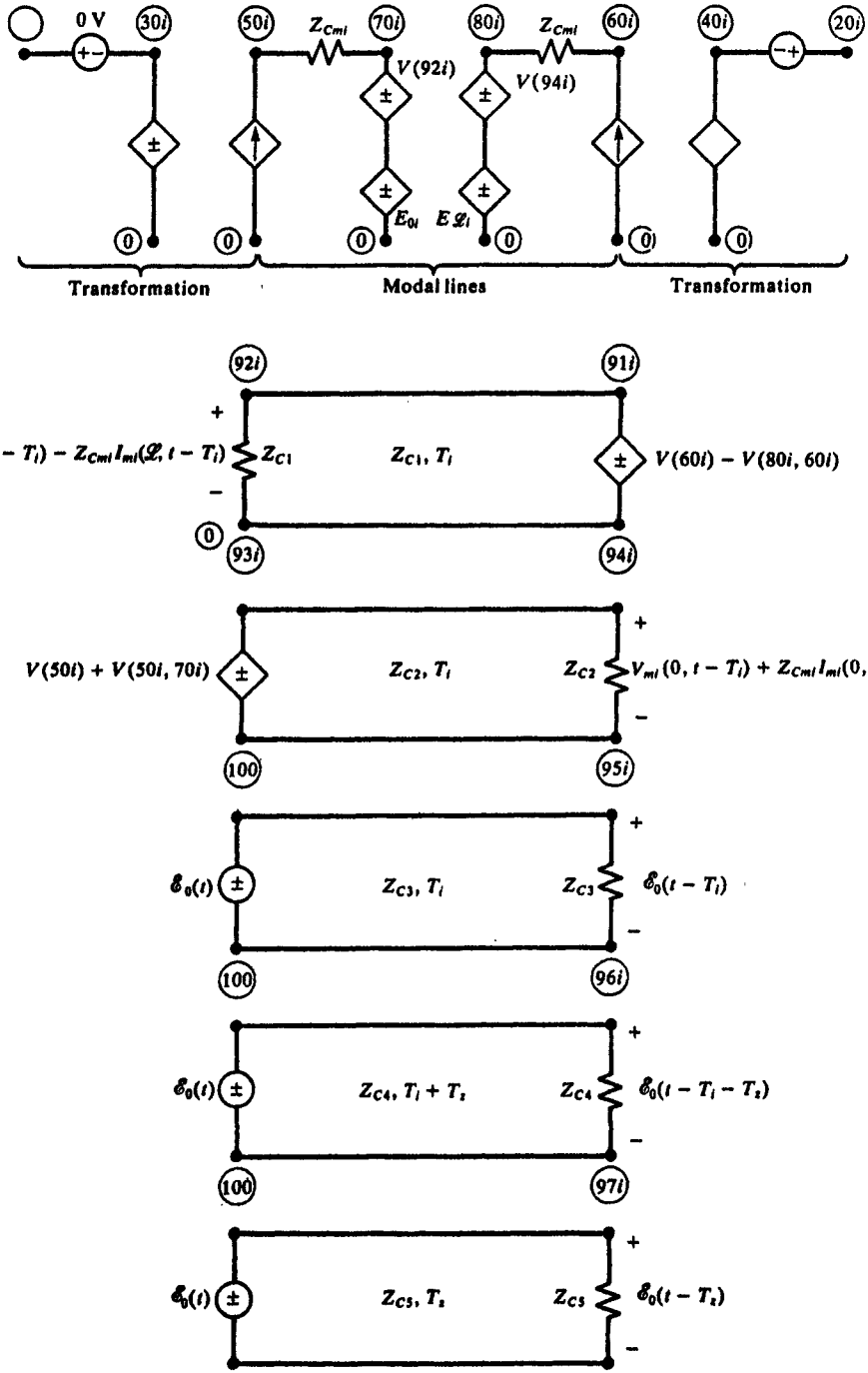

FIGURE 7.23 The SPICE model for a MTL with incident-field illumination.

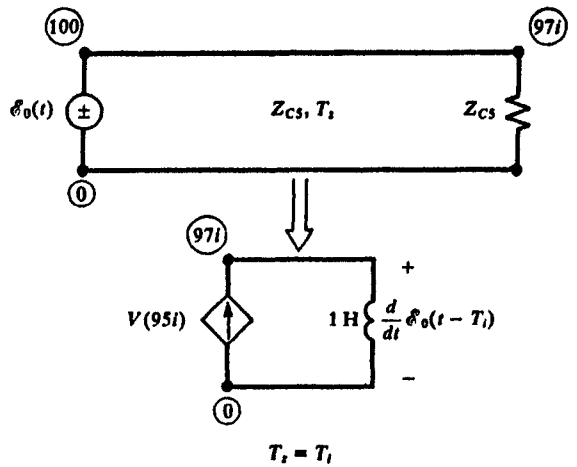

FIGURE 7.24 Replacement of one of the sources in Fig. 7.23 for the special case where the propagation is solely in the z direction and the mode velocity equals that of the incident wave.

waveform with a sufficiently long period. The frequency-domain transfer function can be obtained with the previous methods such as the code **INCIDENT.FOR** described in Appendix A. The magnitudes of the spectral components of $\mathscr{E}_0(t)$ are multiplied by the magnitudes of the transfer function and the phase angles of $\mathscr{E}_0(t)$ are added to the angles of the transfer function to produce the magnitude and phase of the response in the usual fashion. Then the inverse Fourier transform can be used to convert this back to the time domain.

The method is straightforward and can handle $\sqrt{f}$ skin-effect losses. However, it relies on superposition so that the two port must be linear. This again means that the line terminations as well as the surrounding medium must be *linear*. Therefore nonlinear loads as well as corona breakdown in lightning studies cannot be handled with this method.

7.3.2.5 Finite Difference–Time Domain Methods Another straightforward way of solving the MTL equations is with the finite difference–time domain (FDTD) method described in Chapter 5. The FDTD discretization of the transmission-line equations with incident-field illumination was obtained in Chapter 5. Other FDTD derivations and discretizations are given in [8] and [19–21]. The space and time derivatives are discretized as Δz and Δt, respectively, giving a recursion relation in the form of a set of difference equations. The transmission-line equations in (7.18) become

$$\frac{\partial}{\partial z}\mathbf{V}(z, t) + \mathbf{R}\mathbf{I}(z, t) + \mathbf{L}\frac{\partial}{\partial t}\mathbf{I}(z, t) = -\frac{\partial}{\partial z}\mathbf{E}_T(z, t) + \mathbf{E}_L(z, t) + \mathbf{V}'_F(z, t) \quad (7.244a)$$

$$\frac{\partial}{\partial z}\mathbf{I}(z,t)+\mathbf{G}\mathbf{V}(z,t)+\mathbf{C}\frac{\partial}{\partial t}\mathbf{V}(z,t)=-\frac{\partial}{\partial t}\mathbf{C}\mathbf{E}_T(z,t)+\mathbf{I}'_F(z,t) \quad (7.244b)$$

where the $n \times 1$ vectors $\mathbf{E}_T$ and $\mathbf{E}_L$ are due to the transverse and longitudinal components of the incident electric field, respectively. The vectors $\mathbf{V}'_F(z,t)$ and $\mathbf{I}'_F(z,t)$ as well as $\mathbf{R}$ and $\mathbf{G}$ are used to model lumped sources along the line such as at the terminations, as described in Chapter 5. These were given, in the frequency domain, in (7.231) and (7.232). Thus (removing $\sin\psi_k/\psi_k$ and $e^{-j\psi_k}$)

$$\left[-\frac{\partial}{\partial z}\hat{\mathbf{E}}_T(z)+\hat{\mathbf{E}}_L(z)\right]_l=j\omega\left[\frac{1}{v_z}(e_x x_l+e_y y_l)-\left(\frac{x_l}{v_x}+\frac{y_l}{v_y}\right)e_z\right]\hat{E}_o(\omega)e^{-j\beta_z z} \quad (7.245)$$

This translates in the time domain to

$$-\frac{\partial}{\partial z}\mathbf{E}_T(z,t)+\mathbf{E}_L(z,t)=\left(\frac{1}{v_z}\mathbf{A}_T-\mathbf{A}_L\right)\frac{\partial}{\partial z}\mathscr{E}_o\left(t-\frac{z}{v_z}\right) \quad (7.246)$$

where

$$\mathbf{A}_T=\begin{bmatrix}\vdots\\(e_x x_l+e_y y_l)\\\vdots\end{bmatrix} \quad (7.247a)$$

$$\mathbf{A}_L=\begin{bmatrix}\vdots\\\left(\frac{x_l}{v_x}+\frac{y_l}{v_y}\right)e_z\\\vdots\end{bmatrix} \quad (7.247b)$$

Similarly,

$$-\frac{\partial}{\partial t}\mathbf{C}\mathbf{E}_T(z,t)=-\mathbf{C}\mathbf{A}_T\frac{\partial}{\partial t}\mathscr{E}_o\left(t-\frac{z}{v_z}\right) \quad (7.248)$$

The voltage and current solution points are interlaced one half-cell apart as shown in Figs. 5.21 and 5.22 for stability purposes. Similarly, the voltage and current solution times are also interlaced one half-time-step apart as shown in Fig. 5.22. Using this scheme, the difference equations become

$$\frac{1}{\Delta z}(\mathbf{V}_{k+1}^{n+1}-\mathbf{V}_k^{n+1})+\frac{1}{\Delta t}\mathbf{L}(\mathbf{I}_k^{n+3/2}-\mathbf{I}_k^{n+1/2})+\tfrac{1}{2}\mathbf{R}(\mathbf{I}_k^{n+3/2}+\mathbf{I}_k^{n+1/2}) \quad (7.249a)$$

$$=\left(\frac{1}{v_z}\mathbf{A}_T-\mathbf{A}_L\right)\frac{1}{\Delta t}\left[\mathscr{E}_o\left(t^{n+3/2}-\frac{(k-1/2)\Delta z}{v_z}\right)-\mathscr{E}_o\left(t^{n+1/2}-\frac{(k-1/2)\Delta z}{v_z}\right)\right]$$
$$+\tfrac{1}{2}(\mathbf{V}'^{n+3/2}_{Fk}+\mathbf{V}'^{n+1/2}_{Fk})$$

$$\frac{1}{\Delta z}(\mathbf{I}_k^{n+1/2} - \mathbf{I}_{k-1}^{n+1/2}) + \frac{1}{\Delta t}\mathbf{C}(\mathbf{V}_k^{n+1} - \mathbf{V}_k^n) + \tfrac{1}{2}\mathbf{G}(\mathbf{V}_k^{n+1} + \mathbf{V}_k^n) \tag{7.249b}$$

$$= -\mathbf{C}\mathbf{A}_T \frac{1}{\Delta t}\left[\mathscr{E}_o\left(t^{n+1} - \frac{(k-1)\Delta z}{v_z}\right) - \mathscr{E}_o\left(t^n - \frac{(k-1)\Delta z}{v_z}\right)\right]$$

$$+ \tfrac{1}{2}(\mathbf{I}'^{n+1}_{Fk} + \mathbf{I}'^{n}_{Fk})$$

Rearranging these gives

$$\left(\frac{1}{\Delta t}\mathbf{C} + \frac{1}{2}\mathbf{G}\right)\mathbf{V}_k^{n+1} = \left(\frac{1}{\Delta t}\mathbf{C} - \frac{1}{2}\mathbf{G}\right)\mathbf{V}_k^n - \frac{1}{\Delta z}(\mathbf{I}_k^{n+1/2} - \mathbf{I}_{k-1}^{n+1/2}) \tag{7.250a}$$

$$-\mathbf{C}\mathbf{A}_T \frac{1}{\Delta t}\left[\mathscr{E}_o\left(t^{n+1} - \frac{(k-1)\Delta z}{v_z}\right)\right.$$

$$\left. - \mathscr{E}_o\left(t^n - \frac{(k-1)\Delta z}{v_z}\right)\right] + \frac{1}{2}(\mathbf{I}'^{n+1}_{Fk} + \mathbf{I}'^{n}_{Fk})$$

$$\left(\frac{1}{\Delta t}\mathbf{L} + \frac{1}{2}\mathbf{R}\right)\mathbf{I}_k^{n+3/2} = \left(\frac{1}{\Delta t}\mathbf{L} - \frac{1}{2}\mathbf{R}\right)\mathbf{I}_k^{n+1/2} - \frac{1}{\Delta z}(\mathbf{V}_{k+1}^{n+1} - \mathbf{V}_k^{n+1}) \tag{7.250b}$$

$$+ \left(\frac{1}{v_z}\mathbf{A}_T - \mathbf{A}_L\right)\frac{1}{\Delta t}\left[\mathscr{E}_o\left(t^{n+3/2} - \frac{(k-1/2)\Delta z}{v_z}\right)\right.$$

$$\left. - \mathscr{E}_o\left(t^{n+1/2} - \frac{(k-1/2)\Delta z}{v_z}\right)\right] + \frac{1}{2}(\mathbf{V}'^{n+3/2}_{Fk} + \mathbf{V}'^{n+1/2}_{Fk})$$

The terminal conditions are incorporated as before. We characterize these as resistive in the form of generalized Thévenin equivalents as

$$\mathbf{V}(0, t) = \mathbf{V}_S - \mathbf{R}_S\mathbf{I}(0, t) \tag{7.251a}$$

$$\mathbf{V}(\mathscr{L}, t) = \mathbf{V}_L + \mathbf{R}_L\mathbf{I}(\mathscr{L}, t) \tag{7.251b}$$

First the line voltages are solved for from (7.250a). With reference to Fig. 5.21, we let $\mathbf{I}_0 = 0$, $\mathbf{G} = (1/\Delta z)\mathbf{R}_S^{-1}$, $\mathbf{I}'_F = (1/\Delta z)\mathbf{R}_S^{-1}\mathbf{V}_S$ along with replacing $\mathbf{C}$ with $(1/2)\mathbf{C}$ as before for $k = 1$ to yield

$$\mathbf{V}_1^{n+1} = \left(\frac{\Delta z}{\Delta t}\mathbf{R}_S\mathbf{C} + 1\right)^{-1}\left\{\left(\frac{\Delta z}{\Delta t}\mathbf{R}_S\mathbf{C} - 1\right)\mathbf{V}_1^n - 2\mathbf{R}_S\left(\mathbf{I}_1^{n+1/2} - \underbrace{\mathbf{I}_0^{n+1/2}}_{0}\right)\right. \tag{7.252a}$$

$$\left. - \frac{\Delta z}{\Delta t}\mathbf{R}_S\mathbf{C}\mathbf{A}_T[\mathscr{E}_o(t^{n+1}) - \mathscr{E}_o(t^n)] + (\mathbf{V}_S^{n+1} + \mathbf{V}_S^n)\right\}$$

For $k = 2, \ldots, NDZ$ we obtain

$$\mathbf{V}_k^{n+1} = \mathbf{V}_k^n - \frac{\Delta t}{\Delta z}\mathbf{C}^{-1}(\mathbf{I}_k^{n+1/2} - \mathbf{I}_{k-1}^{n+1/2}) \tag{7.252b}$$
$$-\mathbf{A}_T\left[\mathscr{E}_o\left(t^{n+1} - \frac{(k-1)\Delta z}{v_z}\right) - \mathscr{E}_o\left(t^n - \frac{(k-1)\Delta z}{v_z}\right)\right]$$

With reference to Fig. 5.21, we let $\mathbf{I}_{NDZ+1} = 0$, $\mathbf{G} = (1/\Delta z)\mathbf{R}_L^{-1}$, $\mathbf{I}_F' = (1/\Delta z)\mathbf{R}_L^{-1}\mathbf{V}_L$ along with replacing $\mathbf{C}$ with $(1/2)\mathbf{C}$ as before for $k = NDZ + 1$ to yield

$$\mathbf{V}_{NDZ+1}^{n+1} = \left(\frac{\Delta z}{\Delta t}\mathbf{R}_L\mathbf{C} + 1\right)^{-1} \tag{7.252c}$$
$$\times\left\{\left(\frac{\Delta z}{\Delta t}\mathbf{R}_L\mathbf{C} - 1\right)\mathbf{V}_{NDZ+1}^n - 2\mathbf{R}_L\left(\underbrace{\mathbf{I}_{NDZ+1}^{n+1/2}}_{0} - \mathbf{I}_{NDZ}^{n+1/2}\right) - \frac{\Delta z}{\Delta t}\mathbf{R}_L\mathbf{C}\mathbf{A}_T\right.$$
$$\left.\times\left[\mathscr{E}_o\left(t^{n+1} - \frac{NDZ\Delta z}{v_z}\right) - \mathscr{E}_o\left(t^n - \frac{NDZ\Delta z}{v_z}\right)\right] + (\mathbf{V}_L^{n+1} + \mathbf{V}_L^n)\right\}$$

Once the voltages are determined along the line for a particular time step, the currents are obtained from (7.250b) for $k = 1, \ldots, NDZ$ as

$$\mathbf{I}_k^{n+3/2} = \mathbf{I}_k^{n+1/2} - \frac{\Delta t}{\Delta z}(\mathbf{V}_{k+1}^{n+1} - \mathbf{V}_k^{n+1}) + \mathbf{L}^{-1}\left(\frac{1}{v_z}\mathbf{A}_T - \mathbf{A}_L\right) \tag{7.252d}$$
$$\times\left[\mathscr{E}_o\left(t^{n+3/2} - \frac{(k-1/2)\Delta z}{v_z}\right) - \mathscr{E}_o\left(t^{n+1/2} - \frac{(k-1/2)\Delta z}{v_z}\right)\right]$$

Once again, for stability, the position and time discretizations must satisfy the Courant condition:

$$\Delta t \leq \frac{\Delta z}{v_{i\mathrm{MAX}}} \tag{7.253}$$

where $v_{i\mathrm{MAX}}$ is the maximum of the mode velocities.

This method is implemented in the FORTRAN program **FDTDINC.FOR** that is described in Appendix A.

7.3.2.6 Computed Results The computed results compare the SPICE model, the time-domain to frequency-domain transformation, and the finite difference–time domain (FDTD) model. The structure is shown in Fig. 7.25 and consists of a 2 m length of ribbon cable. The wire radii are 7.5 mils, the dielectric

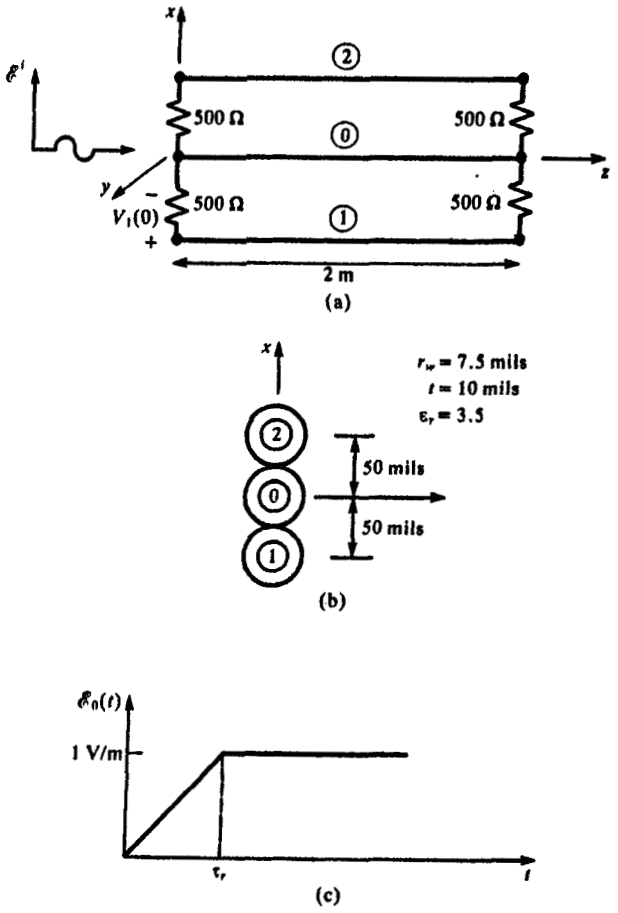

FIGURE 7.25 A three-wire line for illustrating numerical results.

thicknesses are 10 mils and the dielectric constant is 3.5. The wires have center-to-center separations of 50 mils. The middle wire is chosen as the reference conductor, and a uniform plane wave is incident in the z direction with the electric field polarized in the x direction. The line is terminated in 500 Ω resistors giving

$$\mathbf{R}_S = \mathbf{R}_S = \begin{bmatrix} 500 & 0 \\ 0 & 500 \end{bmatrix}$$

The time form of the incident electric field, $\mathscr{E}_0(t)$, is a ramp waveform rising to a level of 1 V/m with various risetimes τ_r = 100 ns, 10 ns, and 1 ns.

It is important to note that the *incident* field should be computed as the field with the conductors removed. Thus, in computing this incident field we should

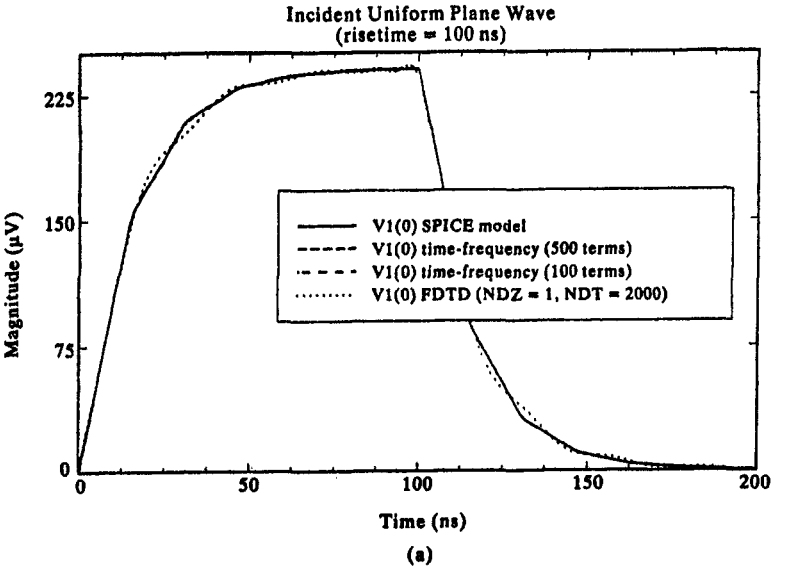

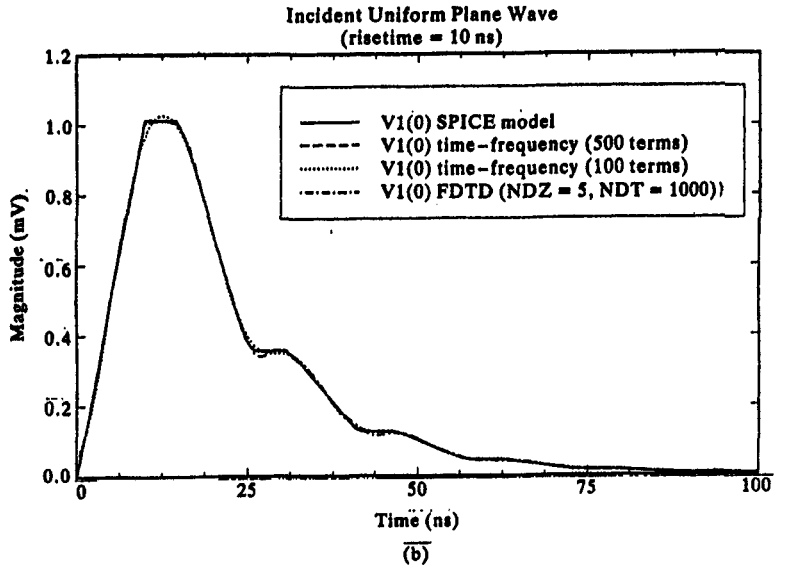

FIGURE 7.26 Predictions of the time-domain near-end voltage of the line of Fig. 7.25 using the SPICE model, the series solution, the time-domain to frequency-domain transformation method, and the FDTD method for an incident uniform plane wave with a risetime of (a) 100 ns, (b) 10 ns, and (c) 1 ns.

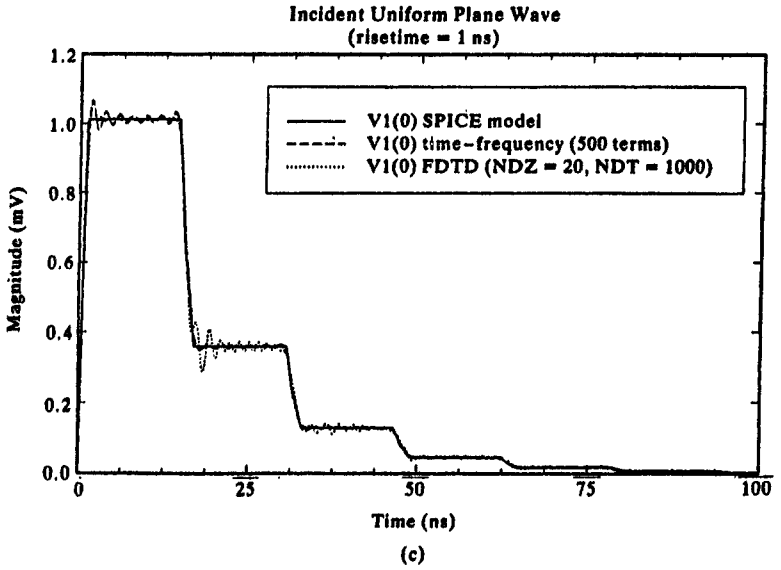

FIGURE 7.26 (*continued*)

leave the dielectric insulations in place. However, to simplify the problem we will assume the incident field to be that with the conductors *and* their insulations removed.

Figure 7.26(a) shows the results for the 100 ns rise time. All three models show excellent correlation. The time-domain to frequency-domain transformation simulated the $\mathscr{E}_0(t)$ waveform as a 1 MHz trapezoidal pulse with a 50% duty cycle and equal rise and fall times. The results were obtained using 100 harmonics and 500 harmonics. The FDTD results were obtained by discretizing the line into $NDZ = 1$ sections of length $\Delta z = \mathscr{L}/NDZ = 2$ m length and the time into $NDT = 2000$ time steps of Δt = final time/$NDT = 0.1$ ns. The spectrum of $\mathscr{E}_0(t)$ rolls off at -40 dB/decade above $1/\pi\tau_r = 3.18$ MHz. Each section is $\lambda/10$ at 15 MHz which is well above the point where the waveform spectrum begins to roll off at -40 dB/decade so the results are not surprising. The results for the 10 ns risetime is shown in Fig. 7.26(b). For the 10 ns risetime, all three models give excellent correlation. The spectrum of $\mathscr{E}_0(t)$ rolls off at -40 dB/ decade above $1/\pi\tau_r = 31.8$ MHz so the time-domain to frequency-domain transformation method using only 100 harmonics gives reasonably accurate results. The FDTD method uses $NDZ = 5$ and $NDT = 1000$. Each section is $\lambda/10$ at 75 MHz which is well above the point where the waveform spectrum begins to roll off at -40 dB/decade so the results are again not surprising. The results for the 1 ns risetime are shown in Fig. 7.26(c). The spectrum of $\mathscr{E}_0(t)$ rolls off at -40 dB/decade above $1/\pi\tau_r = 318$ MHz so the time-domain to frequency-domain transformation method using 500 harmonics gives reasonably accurate results. The FDTD method uses $NDZ = 20$ and

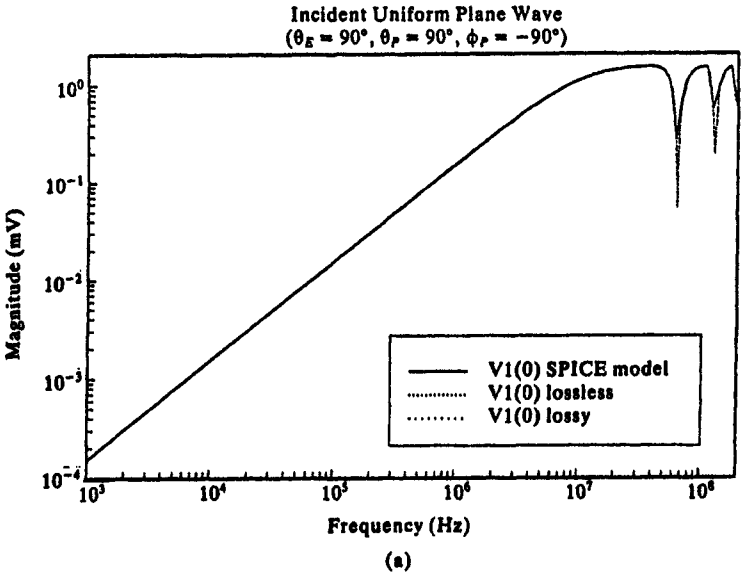

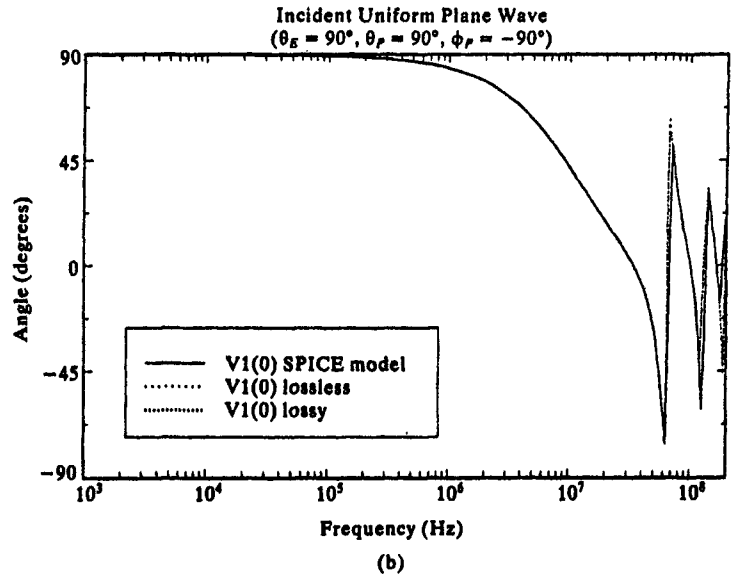

FIGURE 7.27 Predictions of the frequency response of the near-end voltage of the line of Fig. 7.25 using the SPICE model, and the MTL model with and without losses: (a) magnitude, (b) phase. Incident uniform plane wave, $\theta_E = 90°$, $\theta_p = 90°$, $\phi_p = 90°$.

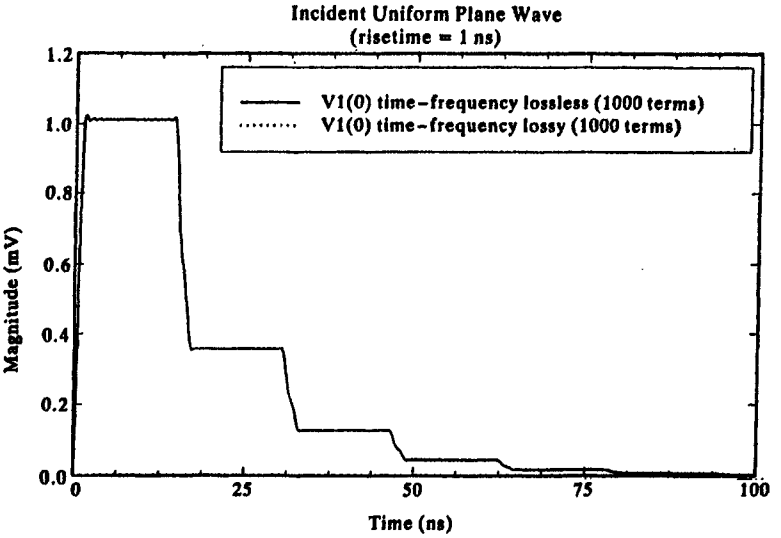

FIGURE 7.28 Predictions of the time-domain near-end voltage of the line of Fig. 7.25 using the time-domain to frequency-domain transformation method with and without losses for an incident uniform plane wave with risetime of 1 ns.

$NDT = 1000$. Each section length, $\Delta z = 0.1$ m, is $\lambda/10$ at 300 MHz which is of the order of the point where the waveform spectrum begins to roll off at -40 dB/decade, so some ringing on that prediction is expected.

The SPICE model is not restricted to the time domain and can be used to give frequency-domain results although restricted to lossless lines. These are shown in Fig. 7.27 from 1 kHz to 200 MHz. The results of the frequency-domain direct calculation with and without losses are obtained using the code **INCIDENT.FOR**. All three models give virtually identical results except around frequencies where the line is some multiple of a half-wavelength.

The effect of losses on the time-domain results can be investigated by computing the results using the time-domain to frequency-domain method using the **TIMEFREQ.FOR** program described in Appendix A. The frequency-domain transfer function is computed with and without losses using the program **INCIDENT.FOR**. The time-domain results for 1 ns risetime are compared in Fig. 7.28 using 1000 harmonics of the 1 MHz waveform. The highest spectral component, 1000 MHz, is a factor of 3 higher than the point the spectrum rolls off at -40 dB/decade, $1/\pi\tau_r = 318$ MHz, so the excellent predictions are to be expected. The results with and without losses are virtually identical. This is not to say that losses are always unimportant, but for the particular load-impedance level, line dimensions, and spectral content of the waveform used here, they are apparently not significant.

REFERENCES

[1] C.D. Taylor, R.S. Satterwhite, and C.W. Harrison, "The Response of a Terminated Two-Wire Transmission Line Excited by a Nonuniform Electromagnetic Field," *IEEE Trans. on Antennas and Propagation*, **AP-13**, 987–989 (1965).

[2] A.A. Smith, Jr., "A More Convenient Form of the Equations for the Response of a Transmission Line Excited by Nonuniform Fields," *IEEE Trans. on Electromagnetic Compatibility*, **EMC-15**, 151–152 (1973).

[3] K.S.H. Lee, "Two Parallel Terminated Conductors in External Fields," *IEEE Trans. on Electromagnetic Compatibility*, **EMC-20**, 288–295 (1978).

[4] S. Frankel, "Forcing Functions for Externally Excited Transmission Lines," *IEEE Trans. on Electromagnetic Compatibility*, **EMC-22**, 210 (1980).

[5] A.A. Smith, *Coupling of External Electromagnetic Fields to Transmission Lines*, 2d ed., Interference Control Technologies, 1987.

[6] F.M. Tesche, T.K. Liu, S.K. Chang, and D.V. Giri, "Field Excitation of Multiconductor Transmission Lines," Technical Report AFWL-TR-78-185, Air Force Weapons Lab, Albuquerque, NM, February 1979.

[7] G.W. Bechtold and D.J. Kozakoff, "Transmission Line Mode Response of a Multiconductor Cable in a Transient Electromagnetic Field," *IEEE Trans. on Electromagnetic Compatibility*, **EMC-12**, 5–9 (1970).

[8] A.K. Agrawal, H.J. Price, and S.H. Gurbaxani, "Transient Response of Multiconductor Transmission Lines Excited by a Nonuniform Electromagnetic Field," *IEEE Trans. on Electromagnetic Compatibility*, **EMC-22**, 119–129 (1980).

[9] C.D. Taylor and J.P. Castillo, "On the Response of a Terminated Twisted-Wire Cable Excited by a Plane-Wave Electromagnetic Field," *IEEE Trans. on Electromagnetic Compatibility*, **EMC-22**, 16–19 (1980).

[10] E.F. Vance, *Coupling to Shielded Cables*, John Wiley & Sons, NY, 1978.

[11] Y. Leviatan and A.T. Adams, "The Response of a Two-Wire Transmission Line to Incident Field and Voltage Excitation, Including the Effects of Higher Order Modes," *IEEE Trans. on Antennas and Propagation*, **AP-30**, 998–1003 (1982).

[12] G.E. Bridges and L. Shafai, "Plane Wave Coupling to Multiple Conductor Transmission Lines Above a Lossy Earth," *IEEE Trans. on Electromagnetic Compatibility*, **31**, 21–33 (1989).

[13] F.M. Tesche, "Plane Wave Coupling to Cables," in *Handbook of Electromagnetic Compatibility*, Academic Press, San Diego, CA, 1994.

[14] J.H. Richmond, "Radiation and Scattering by Thin-Wire Structures in the Complex Frequency Domain," Interaction Note 202, Air Force Weapons Laboratory, Kirtland Air Force Base, Albuquerque, NM, May 1974.

[15] J.H. Richmond, "Computer Program for Thin-Wire Structures in a Homogeneous Conducting Medium," Technical Report, NASA CR-2399, National Aeronautics and Space Administration, Washington, DC, June 1974.

[16] C.W. Harrison, "Generalized Theory of Impedance Loaded Multiconductor Transmission Lines in an Incident Field," *IEEE Trans. on Electromagnetic Compatibility*, **EMC-14**, 56–63 (1972).

[17] F. Schlagenhaufer and H. Singer, "Investigations of Field-Excited Multiconductor Lines with Nonlinear Loads," *Proc. 1990 International Symposium on Electromagnetic Compatibility*, August 1990, Washington, DC, pp. 95–99.

[18] Y. Kami and R. Sato, "Transient Response of a Transmission Line Excited by an Electromagnetic Pulse," *IEEE Trans. on Electromagnetic Compatibility*, EMC-30, 457–462 (1988).

[19] D.E. Meriwether, "A Numerical Solution for the Response of a Strip Transmission Line over a Ground Plane Excited by Ionizing Radiation," *IEEE Trans. on Nuclear Science*, NS-18, 398–403 (1971).

[20] D.F. Higgins, "Calculating Transmission Line Transients on Personal Computers," *IEEE International Symposium on Electromagnetic Compatibility*, August 25–27, 1987, Atlanta, GA.

[21] E.S.M. Mok, and G.I. Costache, "Skin-Effect Considerations on Transient Response of a Transmission Line Excited by an Electromagnetic Pulse," *IEEE Trans. on Electromagnetic Compatibility*, EMC-34, 320–329 (1992).

PROBLEMS

7.1 Derive the relation between the transverse and longitudinal electric fields and the normal magnetic field given in (7.9) from Faraday's law.

7.2 Derive the result for the phasor chain parameter matrix given in (7.29).

7.3 Prove the relation given in (7.36).

7.4 Derive the relations given in (7.42) and (7.43).

7.5 Derive the relations given in (7.47) and (7.48).

7.6 Derive the relations given in (7.49) and (7.50).

7.7 Derive the relations given in (7.51) and (7.52).

7.8 Derive the result for a lossless line in a homogeneous medium given in (7.57).

7.9 Derive the relations given in (7.59).

7.10 Derive the relations given in (7.66) and (7.67).

7.11 Derive the relations given in (7.78).

7.12 Derive the relations given in (7.89) and (7.90).

7.13 Derive the relations given in (7.93) and (7.94).

7.14 Derive the relations given in (7.100) and (7.101).

7.15 Derive the relations given in (7.106) and (7.107).

7.16 Consider a two-wire line consisting of two #20 gauge (radius 16 mils) bare wires separated by 5 cm and total length 5 m. The loads are 50 Ω

at $z = 0$ and $1000\,\Omega$ at $z = \mathscr{L}$. Sketch the frequency response of the voltage across each load from 1 kHz to 100 MHz for a 1 V/m incident field that has $\theta_E = 60°$, $\theta_p = 120°$, $\phi_p = -30°$. Compare the exact results to the electrically short line model of Section 7.2.5.4 which predicts a 20 dB/decade variation for all frequencies.

7.17 Repeat Problem 7.16 replacing the reference wire with an infinite ground plane.

7.18 Repeat Problem 7.16 replacing the two wires with a PCB having two 10 mil lands of length 10 cm separated by 50 mils. The board is constructed of glass epoxy ($\varepsilon_r = 5$) and is 64 mils thick.

7.19 Derive the solution given in (7.163).

7.20 Derive the series solutions given in (7.169).

7.21 Derive the relations given in (7.200).

7.22 Derive the modal chain parameter matrices given in (7.220).

7.23 Derive the modal forcing functions given in (7.237) and (7.240).

7.24 Derive the functions given in (7.245) to (7.247).

7.25 Derive the difference equations given in (7.252).

7.26 Repeat Problem 7.16 but obtain the time-domain response using:

1. The SPICE model
2. The time-domain to frequency-domain model
3. The FDTD model

The incident waveform is a periodic "sawtooth" wave rising from zero to its maximum in $\tau_r = 200\,ns$ and returning to zero in $\tau_f = 50\,ns$. Compare these to the electrically short line model of Section 7.3.1.4.

7.27 Repeat Problem 7.26 replacing the reference wire with an infinite ground plane.

7.28 Repeat Problem 7.26 replacing the two wires with a PCB having two 10 mil lands of length 10 cm separated by 50 mils. The board is constructed of glass epoxy ($\varepsilon_r = 5$) and is 64 mils thick.